Energy Conversion and Management 372 (2027) 122283

Contents lists available at ScienceDirect

Energy Conversion and Management

journal homepage: www.elsevier.com/locate/enconman

Research paper

Future hydrogen demand in Europe's steel and chemical sectors: A site-specific assessment

Anthony Britto *, Leonie Gröning, Leandra Scharnhorst, Max Kleinebrahm, Wolf Fichtner

Institute for Industrial Production, Karlsruhe Institute of Technology (KIT), Hertzstr. 16 – Building 06.33, 76187 Karlsruhe, Germany

ARTICLE INFO

Dataset link: https://gitlab.kit.edu/kit/iip/opensource/forecast-sites-ext

Keywords:
Industrial decarbonisation
Hydrogen demand
Steel industry
Chemical industry
Site-specific modelling
European hydrogen backbone

ABSTRACT

Hydrogen is expected to play a central role in decarbonising Europe's steel and chemical industries, but future demand remains uncertain because technology adoption depends on plant characteristics, infrastructure access, and evolving prices. This study develops an open-source, site-specific assessment of hydrogen demand in Europe's primary steel sector and selected chemical subsectors: ammonia, methanol, and high-value chemicals. Building on the FORECAST-Sites framework, the model combines plant-level production data, techno-economic process assumptions, and the planned European Hydrogen Backbone to simulate investment, reinvestment, shutdown, and hydrogen-connection decisions at individual sites. Within the hydrogen-centred technology portfolio considered, hydrogen demand remains limited through the 2030s but rises sharply after 2040 as large primary steel assets switch to hydrogen-based direct reduction. In the baseline, total demand increases from 23 TWh/y in 2040 to 315 TWh/y in 2050, with steel accounting for 81% of final demand. Chemical hydrogen use emerges earlier but remains smaller, concentrated mainly in ammonia and methanol, while H_2-based methanol-to-olefins remains comparatively uncompetitive in high-value chemicals. Demand is also spatially concentrated, with Germany becoming the dominant demand centre. Overall, aggregate hydrogen-demand projections mask substantial sectoral and spatial heterogeneity, with important implications for infrastructure planning and industrial policy.

1. Introduction

Achieving climate neutrality in Europe requires profound transformations of energy- and emission-intensive industrial sectors. Within the framework of the European Green Deal and the Fit-for-55 package, the European Union aims to reduce greenhouse gas emissions by at least 55% by 2030 and achieve climate neutrality by 2050 [1]. Despite substantial progress in the decarbonisation of the electricity sector, industry remains responsible for approximately 20% of European greenhouse gas emissions and therefore represents a key challenge for long-term climate mitigation efforts. Among industrial sectors, steel and chemicals play a particularly important role due to their high energy demand, substantial process-related emissions, and strategic importance for European value chains: Rozsai et al. document the substantial energy use and emissions associated with European steel and chemical production [2], whereas Lerede et al. [3] further characterise the process-level energy and emissions profiles of these energy-intensive industries.

These industries are characterised by strong fossil-fuel dependence, process-specific technological requirements, and long investment cycles, making their transition toward climate neutrality especially challenging; at the same time, both sectors are expected to become major consumers of low-carbon hydrogen [3]. In primary steel production, hydrogen-based direct reduction followed by electric arc furnace steelmaking is widely regarded as one of the most promising pathways for deep decarbonisation [4]. In the chemical industry, hydrogen plays a dual role as both an energy carrier and a feedstock, particularly in the production of ammonia, methanol, and high-value chemicals [3]. Consequently, hydrogen is frequently identified as a key enabling technology for industrial decarbonisation [5].

However, the future deployment of hydrogen-based production technologies remains highly uncertain. Their competitiveness depends on a range of interacting factors, including hydrogen, electricity, and carbon prices, capital costs, and infrastructure availability [6]. Industrial transformation is further constrained by long-lived production assets and capital-intensive reinvestment cycles [7]. Existing facilities are often operated for several decades, creating path dependencies that

* Corresponding author.
E-mail address: anthony.britto@kit.edu (A. Britto).

https://doi.org/10.1016/j.enconman.2026.122283
Received 17 June 2026; Received in revised form 3 October 2026; Accepted 10 October 2026
Available online 29 October 2026
0196-8904/© 2026 The Authors. Published by Elsevier Ltd. This is an open access article under the CC BY license (http://creativecommons.org/licenses/by/4.0/).
Open access funding enabled and organized by Projekt DEAL.

can either delay or accelerate technology adoption depending on future economic conditions: Bauer and Fontenit [8] show how long-lived petrochemical assets can create carbon lock-in in plastics production, whereas Bachorz et al. [9] demonstrate similarly that the timing of green investment is critical for avoiding carbon lock-in in steel. These challenges are amplified by the spatial heterogeneity of industrial production. Sites differ substantially with respect to technology portfolios, production capacities, plant age structures, regional energy prices, and access to future hydrogen infrastructure [4]. As a result, otherwise identical technologies may become economically attractive at different locations and at different points in time. Future hydrogen demand therefore depends not only on technology costs, but also on site-specific investment opportunities and infrastructure accessibility.

Many existing industrial energy models represent industry at aggregated sectoral or national levels and therefore cannot fully capture these dynamics. Capros et al. [10] analyse EU decarbonisation using the economy-wide PRIMES model. Fleiter et al. [11] develop the bottom-up FORECAST model for analysing industrial energy transitions at sectoral and process level. Guminski [12] evaluates scenario-based transformation pathways and technical abatement measures for European industry. Such approaches provide detailed system- or sector-level insights but do not primarily resolve heterogeneous investment decisions at individual industrial sites. Furthermore, many industrial modelling frameworks rely on proprietary datasets, limiting transparency, reproducibility, and methodological extension. Recent work has begun to address these limitations from different directions: for instance, Schneider [4] develops a spatially explicit model of steel production clusters in Northwestern Europe; Neuwirth et al. [13] model hydrogen-based steel and basic chemical diffusion at individual European production sites; Lerede et al. [14] contribute an open-source and open-data energy-system model for Europe; and Genge et al. [15] analyse alternative green value chains for European basic chemicals using a spatially explicit approach. Together, these studies demonstrate the growing importance of spatial and technological detail in modelling industrial transformation, although explicit links between site-level investment decisions and evolving hydrogen infrastructure remain comparatively limited.

The present study builds on these recent advances in site-specific industrial modelling and contributes to three related strands of literature. First, it relates to technology-rich bottom-up and energy-system models that analyse industrial decarbonisation pathways using detailed process representations [3,11,16]. Second, it contributes to the growing literature on hydrogen-based decarbonisation in steel and chemicals, which identifies hydrogen as a central option for achieving deep emissions reductions in these sectors [4,17,18]. Third, it extends recent site-specific modelling approaches that emphasise the importance of plant-level heterogeneity, reinvestment timing, and infrastructure availability for technology diffusion [13,19].

To this end, the study extends the open-source FORECAST-Sites framework developed by [19]. The model is enhanced through additional site-level industrial data, methodological improvements to technology-adoption decisions, and an explicit representation of hydrogen infrastructure availability based on the planned European Hydrogen Backbone network. Unlike centralised least-cost approaches, technology adoption emerges from modelled heterogeneous site-level investment decisions that account for expected economic attractiveness, reinvestment timing, premature technology replacement, plant closure decisions, and hydrogen connection costs. To ensure transparency and reproducibility, both the model code and the underlying datasets are made fully open source and publicly available through a dedicated repository (https://gitlab.kit.edu/kit/iip/opensource/forecast-sites-ext).

Using this framework, the study investigates future hydrogen demand in Europe's primary steel industry and selected chemical subsectors, namely ammonia, methanol, and high-value chemicals, as a feasibility assessment of potential technology diffusion under specified techno-economic conditions. The analysis provides three main contributions. First, it offers a consistent cross-sector assessment of future hydrogen demand across steel and chemicals under a common modelling framework. Second, it explicitly links technology adoption to site-specific characteristics, reinvestment cycles, and hydrogen infrastructure accessibility. Third, it evaluates the sensitivity of hydrogen demand trajectories to alternative assumptions regarding hydrogen, energy, and carbon prices. The resulting analysis provides insights into both the magnitude and spatial distribution of future industrial hydrogen demand in Europe and highlights the conditions under which hydrogen-based production pathways become economically attractive.

2. Methodology

This section details the methodological approach. We begin with an overview of the model in Section 2.1, followed by a mathematical description of the algorithm developed for site-specific process choice in Section 2.2. Then, Sections 2.3–2.5 detail the industrial site data, process data, and energy-price data used in the scenario modelling.

2.1. Model overview

FORECAST-Sites is a spatially explicit, agent-based simulation model developed by [19] to analyse technological change in energy-intensive industries at a high spatial resolution. The model links site-specific industrial data with techno-economic process parameters and represents transformation dynamics at the level of individual production locations. Its empirical basis is a SQLite database containing harmonised information on industrial sites, production units, process technologies, and energy-related characteristics. An overview of the model is shown in Fig. 1.

Several core aspects of the original FORECAST-Sites investment logic were substantially extended within the present analysis. In the original model, investment decisions followed a simple replacement rule: once a production unit reached the end of its technical lifetime, it was replaced by the cheapest available production process. The present work introduces two additional decision options that are particularly relevant in the context of industrial decarbonisation. First, production units may shut down if reinvestment is no longer economically attractive. Second, units may invest before reaching the end of their technical lifetime if an early technology switch is economically beneficial. In addition, the representation of hydrogen infrastructure costs was refined considerably: the extended model explicitly accounts for pipeline distance, connection type, and available capacity when determining site-specific hydrogen connection costs. These methodological extensions are described in detail below. Moreover, a browser-based frontend was developed to make FORECAST-Sites Extended accessible and interactive. It enables users to configure model inputs, run scenarios, and explore results through maps, charts, and summary visualisations.

FORECAST-Sites Extended is organised into four analytical levels: region, site, production unit, and process. The regional level defines external framework conditions, including energy-carrier prices, taxes, subsidies, energy-carrier availability, and scenario-wide parameters such as the carbon price. Sites correspond to individual geographical production locations and provide the spatial reference for infrastructure-related variables, such as proximity to hydrogen pipelines. Production units are the core decision-making entities of the model. Each unit represents a production asset at a given site and is characterised by its product, installed process, production volume, and year of last reinvestment. This structure captures both the technological composition and age structure of the existing industrial capital stock. At the process level, the model defines the feasible production routes for each product and assigns process-specific parameters, including capital expenditure, operating expenditure, technical lifetime, energy and feedstock demand, steam demand, and process-related emissions. The bottom-up structure captures heterogeneity in existing capital stock, production technologies, energy prices, and infrastructure access,

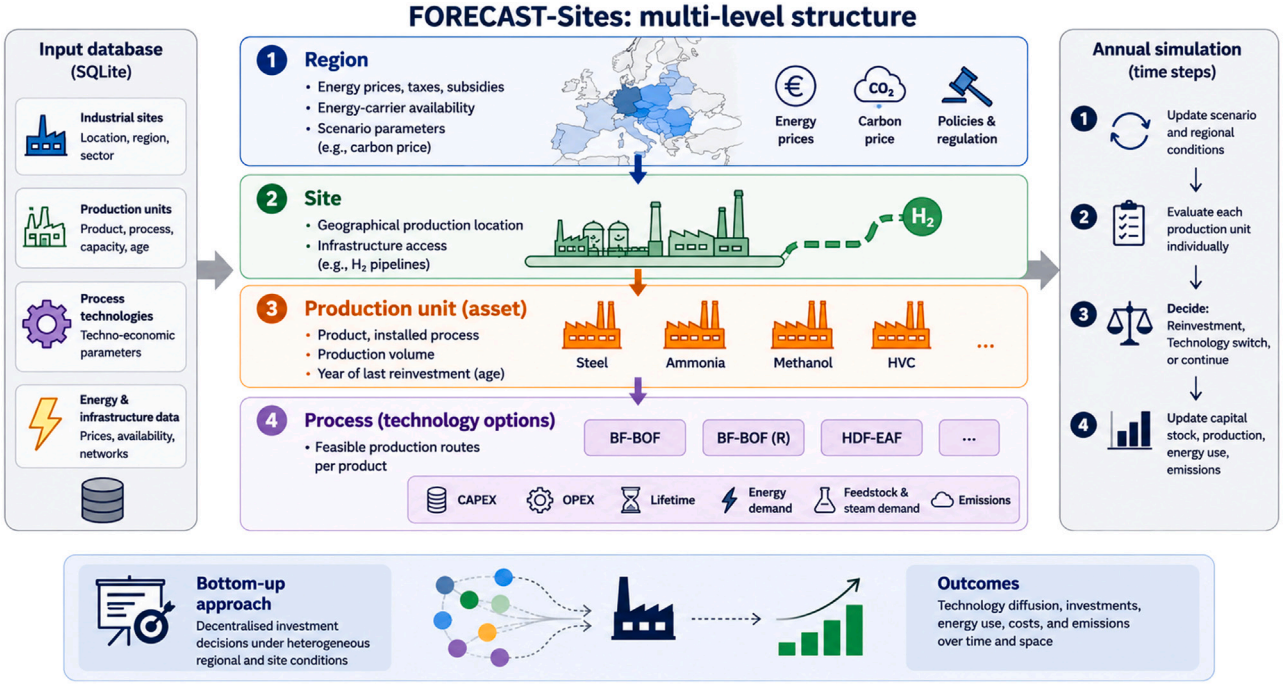


Fig. 1. Schematic overview of the FORECAST-Sites model.
Source: Adapted from [19].

which is particularly relevant for infrastructure-dependent hydrogen technologies.

The simulation proceeds in annual time steps. In each year, regional and scenario conditions are updated, after which each production unit is evaluated with respect to reinvestment, technology switching, and economic feasibility. The model therefore captures both end-of-lifetime reinvestment and premature replacement when alternative processes become economically attractive.

2.2. Site-level process choice

A schematic of the production unit's investment logic, which is evaluated for each simulation year, is shown in Fig. 2. Let t denote the current simulation year, p_t the process currently installed in the unit, Q the annual production volume, and y^{last} the year of the last reinvestment. Each process p has a technical lifetime L_p, so that the end-of-life year of the current unit is

$$y^{\text{EOL}} = y^{\text{last}} + L_{p_t} \,. \tag{1}$$

If $t \geq y^{\text{EOL}}$, reinvestment or shutdown is mandatory. If $t < y^{\text{EOL}}$, the unit may either continue operating the current process or switch early to a cheaper alternative, subject to an economic threshold.

For each available process $p \in \mathcal{P}_t$, the model computes a discounted replacement-chain cost over a common planning horizon H_t,

$$H_t = \operatorname{lcm}\{L_p : p \in \mathcal{P}_t\} \,; \tag{2}$$

here, $\mathcal{P}_t$ is the set of processes whose energy requirements can be met in year t. The replacement-chain cost of investing in process p in year t is given by

$$C_p(t, H_t) = K_p^{\text{pipe}}(t) + \sum_{\substack{\tau=0 \\ \tau \equiv 0 \pmod{L_p}}}^{H_t-1} \frac{Q\, k_p(t+\tau)}{(1+r_p)^\tau} + \sum_{\tau=0}^{H_t-1} \frac{Q\, c_p^{\text{op}}(t+\tau)}{(1+r_p)^\tau} \,, \tag{3}$$

where $k_p(t)$ is CAPEX per tonne of annual capacity, r_p is the process-specific discount rate, and $K_p^{\text{pipe}}(t)$ is a one-time hydrogen pipeline connection cost, applied only to hydrogen-using processes and omitted once the unit is already connected.

Pipeline costs are computed at site level from the distance to the nearest available hydrogen-compatible pipeline. The model first identifies all pipelines that are available in year t, accounting for commissioning year and assumed build or conversion delays, and selects the closest active pipeline to the site. The one-time connection cost is then

$$K_p^{\text{pipe}}(t) = \begin{cases} f_{m,z}\, d_i(t), & \text{if process } p \text{ uses hydrogen and site } i \text{ is not yet connected,} \\ 0, & \text{if site } i \text{ is already connected,} \\ \infty, & \text{if no suitable pipeline is available.} \end{cases} \tag{4}$$

Here, $d_i(t)$ is the great-circle distance in kilometres from site i to the closest available pipeline, $m \in \{\text{H}_2, \text{Gas}, \text{Mix}\}$ is the pipeline mode, and $z \in \{\text{Small}, \text{Medium}, \text{Large}\}$ is the required capacity category of the site. The category z is determined from the site's aggregate potential hydrogen demand, while the cost factor $f_{m,z}$ is specified in €/km and differs between new hydrogen pipelines, repurposed gas pipelines, and mixed cases. Once any production unit at a site has connected to hydrogen infrastructure, the connection is treated as sunk and subsequent hydrogen investments at the same site do not incur an additional pipeline connection cost.

Lastly, the annual operating cost per tonne in (3) is defined as

$$c_p^{\text{op}}(t) = c_p^{\text{base}}(t) + c_p^{\text{energy}}(t, Q) + \pi_t^{\text{CO}_2} \left(e_p^{\text{proc}} + e_p^{\text{energy}}(t)\right) - s_p(t) + x_p(t) \,, \tag{5}$$

where c_p^{base} is non-energy OPEX, c_p^{energy} includes energy, steam and feedstock costs, $\pi_t^{\text{CO}_2}$ is the CO_2 price, e_p^{proc} and e_p^{energy} are process and energy-related emissions intensities, and s_p and x_p denote energy-carrier subsidies and taxes, respectively. Consequently, the cheapest available process in year t is given by

$$p_t^* = \arg\min_{p \in \mathcal{P}_t} C_p(t, H_t) \,. \tag{6}$$

If the unit has not yet reached end of life and the current process is already cost-minimising, $p_t^* = p_t$, no early switch is made. Otherwise, the model evaluates whether switching immediately is preferable to waiting. Early retirement of the current process incurs a stranded-capital

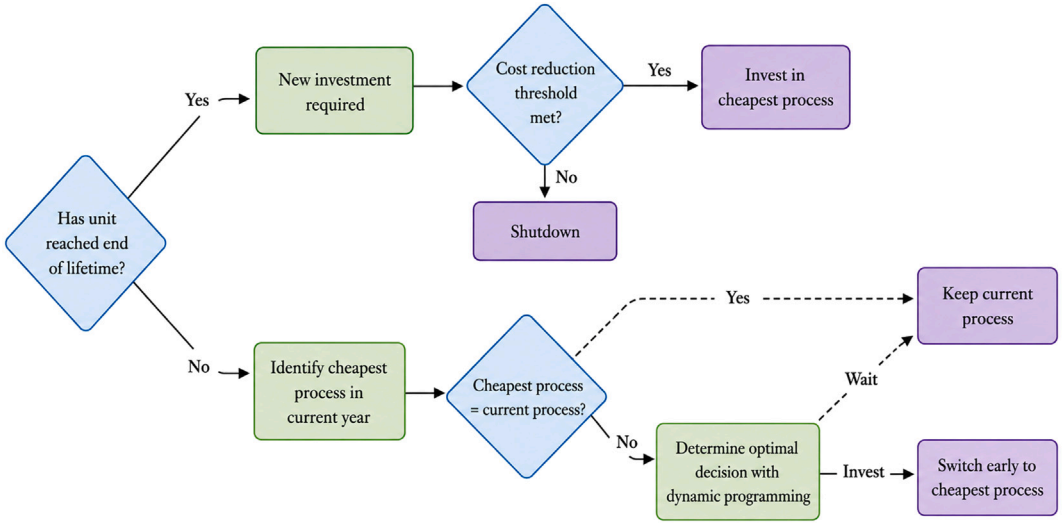


Fig. 2. Schematic of the process-choice logic.

term:

$$S_t = \begin{cases} Q\, k_{p_t}(y^{\text{last}}) \dfrac{y^{\text{EOL}} - t}{L_{p_t}}, & t < y^{\text{EOL}}, \\ 0, & t \geq y^{\text{EOL}} . \end{cases} \tag{7}$$

The immediate-investment value is therefore given by

$$I_t = C_{p_t^*}(t, H_t) + S_t . \tag{8}$$

On the other hand, the value of waiting is computed recursively by dynamic programming. Let V_u be the minimum discounted cost from year u onward, conditional on retaining the current process up to year u. The terminal year is $T = y^{\text{EOL}}$, with terminal condition

$$V_T = C_{p_T^*}(T, H_T) . \tag{9}$$

For years $u = T-1, \ldots, t+1$, the model compares the value of switching in year u, namely I_u, with the value of waiting one additional year,

$$W_u = Q\, c_{p_t}^{\text{op}}(u) + \frac{V_{u+1}}{1 + r_{p_t}} . \tag{10}$$

The Bellman recursion is defined as

$$V_u = \begin{cases} I_u, & \dfrac{I_u}{W_u} < 1 - \theta , \\ W_u, & \dfrac{I_u}{W_u} \geq 1 - \theta , \end{cases} \tag{11}$$

where $0 < \theta < 1$ is a cost-reduction threshold. Thus, early switching is allowed only if immediate investment reduces discounted costs by at least a factor $1-\theta$ relative to waiting. This "early-switching threshold" is introduced to prevent marginal cost differences from causing excessively frequent technology changes. The dynamic program terminates by computing the decision in the current year,

$$W_t = Q\, c_{p_t}^{\text{op}}(t) + \frac{V_{t+1}}{1 + r_{p_t}} , \tag{12}$$

and the unit switches early if

$$\frac{I_t}{W_t} < 1 - \theta . \tag{13}$$

If this condition is not satisfied, the unit keeps its current process for at least one more year.

At the end of life, the cheapest available replacement process is adopted unless the replacement cost is sufficiently unfavourable relative to the current process, in which case the unit is shut down. Similarly to θ, a "reinvestment threshold" $0 < \eta < 1$ is introduced here as well: if the ratio of the replacement costs to current costs exceeds $1-\eta$, the available processes are deemed too expensive relative to the status quo, and the unit is shut down. Economically, this is meant to represent competitive pressure, which encourages industrial producers to continually reduce costs. After a successful investment, the unit state is updated such that $p_{t+1} = p_t^*$ and $y^{\text{last}} = t$.

2.3. Industrial-site & hydrogen-network data

The analysis combines plant-level information for the primary steel and chemical sectors. For primary steel, site-level information was compiled from open industrial plant inventories and sectoral statistics. The main data source is the open-source Global Iron and Steel Tracker, which provides plant-level information on steel production sites, including location, operating status, production route, production capacity, and technology type [20]. The raw data were restricted to active production sites in the European study region and harmonised by standardising plant names, technology labels, capacity units, and country identifiers. Each production unit was assigned to a site and process route, allowing multi-unit industrial complexes to be represented consistently within the model. The resulting primary steel dataset contains 49 production units spread across 23 sites. These data were complemented with European steel-sector statistics and energy-system databases for validation, with the resulting total capacity of 90.42 Mt/yr closely aligning with the 93.44 Mt/yr reported by JRC-IDEES for 2023 [2].

For chemicals, the primary data source is the Global Chemicals Inventory (GCI), which provides plant-level information on 100 production units across 73 European production sites for high-value chemicals (HVCs), ammonia, and methanol [21]. The database reports plant locations, products, and feedstocks, but does not include production capacities, plant ages, or years of last modernisation. These variables were therefore supplemented using the site-level database developed by [13]. The chemical site data were linked to the supplementary site database using geographic coordinates. The spatial matching procedure between the GCI and [13] identified 56 common chemical sites, corresponding to 83 production units. The remaining 17 unmatched sites each contain a single production unit. For 12 of these sites, production capacities were reconstructed from publicly available company information and project reports. For the remaining 5 sites, capacities were estimated from EU ETS emissions data using process-specific emission factors:

$$Q_u = \frac{\text{CO}_{2,\text{total}}}{EF}, \tag{14}$$

where Q_u denotes production volume, $CO_{2,total}$ site-level CO_2 emissions, and EF the process-specific emission factor. To ensure consistency with the FORECAST-Sites modelling framework, the resulting plant counts follow the production-unit assumptions in [13], yielding 53 HVC, 38 ammonia, and 9 methanol production units across 73 sites. In capacity terms, approximately 90% of HVC production capacity is based on data from [13], while 3% is reconstructed from EU ETS emissions and 7% from publicly available company and project information. The corresponding shares for ammonia are approximately 85%, 14%, and 1%, respectively. For methanol, approximately 66% of capacity is based on [13] and 34% on publicly available company and project information. As aggregate plausibility checks, the resulting sectoral capacities were compared with available independent statistics. The modelled ammonia capacity of 13.84 Mt/yr was compared with 18.1 Mt/yr of fertiliser production reported by Fertilizers Europe [22], while the modelled methanol capacity of 2.33 Mt/yr compares well with an initial EU capacity of approximately 2.25 Mt/yr implied by European Commission data [23]. The modelled HVC capacity of 20.76 Mt/yr, for which ethylene serves as the representative process proxy, is close to an initial EU ethylene capacity of approximately 21.4 Mt/yr implied by recent European Commission data [23]. These comparisons provide order-of-magnitude checks rather than exact validation, given differences in product definitions, geographical coverage, and reference years.

Hydrogen network availability is represented using data from the European Hydrogen Backbone (EHB), a consortium-led infrastructure scenario developed by European gas transmission system operators [6,24]. The EHB provides a geospatially explicit outlook for a future European hydrogen transport network, including projected pipeline corridors, commissioning years, and distinctions between newly built hydrogen pipelines and repurposed natural gas infrastructure. In addition, the EHB reports techno-economic assumptions for different pipeline types, including capital expenditure and fixed operating expenditure. These data are used to approximate the timing and spatial availability of hydrogen pipeline access for industrial sites. In the model, each site is therefore evaluated relative to the nearest available EHB pipeline segment in a given year, allowing hydrogen infrastructure constraints to be represented at the site level rather than only through national or regional assumptions.

Fig. 3 provides a spatial overview of the industrial sites included in the analysis and their relation to the projected European hydrogen network in 2050. The site markers represent the primary steel and chemical production facilities considered in the model, while the pipeline layers indicate the hydrogen infrastructure corridors reported by the European Hydrogen Backbone. The figure illustrates the strong spatial clustering of industrial demand around existing production regions, as well as the uneven proximity of sites to future hydrogen transport infrastructure. It therefore highlights why hydrogen availability is treated as a site-specific constraint rather than as a purely national or sectoral assumption.

2.4. Process data

Tables 1 and 2 summarise the techno-economic and process-input assumptions used in the analysis. To ensure a consistent representation across all sectors, the recent assessment by [16] serves as the primary data source, while values from [3] were used as a cross-check where appropriate. Rather than adopting the full set of pathways considered by [16], the analysis focuses on a reduced set of conventional, retrofit, and hydrogen-based production routes that are most relevant to the research objective of assessing future hydrogen demand. This simplification avoids introducing additional competing decarbonisation options while retaining the key technological choices required to represent a hydrogen-centred transition. Throughout this article, all monetary quantities are reported in constant 2021 euros; where inflation adjustment of the original data was necessary, the Industrial Producer Price Index from Eurostat was used [25]. Across sectors, hydrogen-based routes generally substitute fossil-energy and feedstock inputs with electricity and hydrogen, while often requiring higher capital expenditure. These differences in process and feedstock requirements underpin the sector-specific hydrogen-demand patterns analysed below.

2.5. Energy-price data

Electricity and natural gas prices are represented using a dynamic factor model, which captures common movements across countries while preserving country-specific price differences [26].[1] Given the increasing integration of European energy markets, all national time series are modelled jointly rather than independently. Historical industrial electricity and gas prices are taken from Eurostat and include taxes, levies, and surcharges [27,28]. Fig. 4 provides a visual summary for four large industrial countries: Germany, France, Italy, and Spain. The data show pronounced short-run volatility, particularly during the recent energy-price crisis, but also clear visual evidence of mean reversion in both electricity and gas prices. This is consistent with the theoretical expectation that energy prices fluctuate around long-run equilibrium relationships, while still allowing for persistent cross-country differences due to heterogeneity in generation mixes, taxation, network charges, and industrial tariff structures.

Naphtha prices are treated separately, as naphtha is a refinery-derived petroleum product and therefore follows oil-market rather than power- or gas-market dynamics. Historical naphtha prices were taken from U.S. commodity-market data, aggregated from daily to annual observations, converted from US$/t to €/t using annual exchange rates, and deflated to constant 2021 euros [29]. Future prices were then modelled using an ARMA process fitted to the historical annual price series, allowing naphtha prices to revert toward their long-run mean rather than follow a deterministic trend. For implementation, prices were converted to €/GJ using a lower heating value of 44.38 GJ/t. This results in a uniform naphtha price assumption of approximately €10.71/GJ across all EU countries from 2030 onward, reflecting the assumption that naphtha is traded on an integrated international commodity market rather than determined by country-specific industrial energy-price structures.

Coal and EU ETS prices are taken from the TYNDP scenario framework [30]. The EU ETS price is assumed to increase linearly from €8/tCO_2 in 2015 to €168/tCO_2 by 2050, and is applied uniformly across all model regions. Hydrogen prices are based on the corridor-specific supply-cost estimates reported by [6]. The EHB supply corridors are mapped to individual countries; where multiple corridors pass through a country, the arithmetic mean of the relevant corridor prices is used. Low and high price trajectories are available for 2030 and 2040, and a medium (baseline) scenario is constructed as their arithmetic mean. Across the EHB supply corridors, hydrogen prices range from approximately €1,400/t H_2 in the low-cost 2040 scenario to €4,500/t H_2 in the high-cost 2030 scenario, corresponding to roughly €12–38/GJ after conversion to energy units. Values for the other modelled years are then obtained by exponential extrapolation from the 2030 and 2040 data points, reflecting the assumption that long-run hydrogen-cost reductions are driven by relative learning effects rather than constant absolute declines. For non-EU countries in the model domain, hydrogen prices are approximated using the nearest neighbouring EU country covered by the EHB corridor system. This approximation introduces additional uncertainty for non-EU sites, for which the assigned hydrogen price may not fully reflect local supply conditions.

[1] Full technical documentation of the dynamic factor model, including factor selection, country-specific loadings, model estimation, and out-of-sample forecast evaluation, is provided in the accompanying open-source repository.

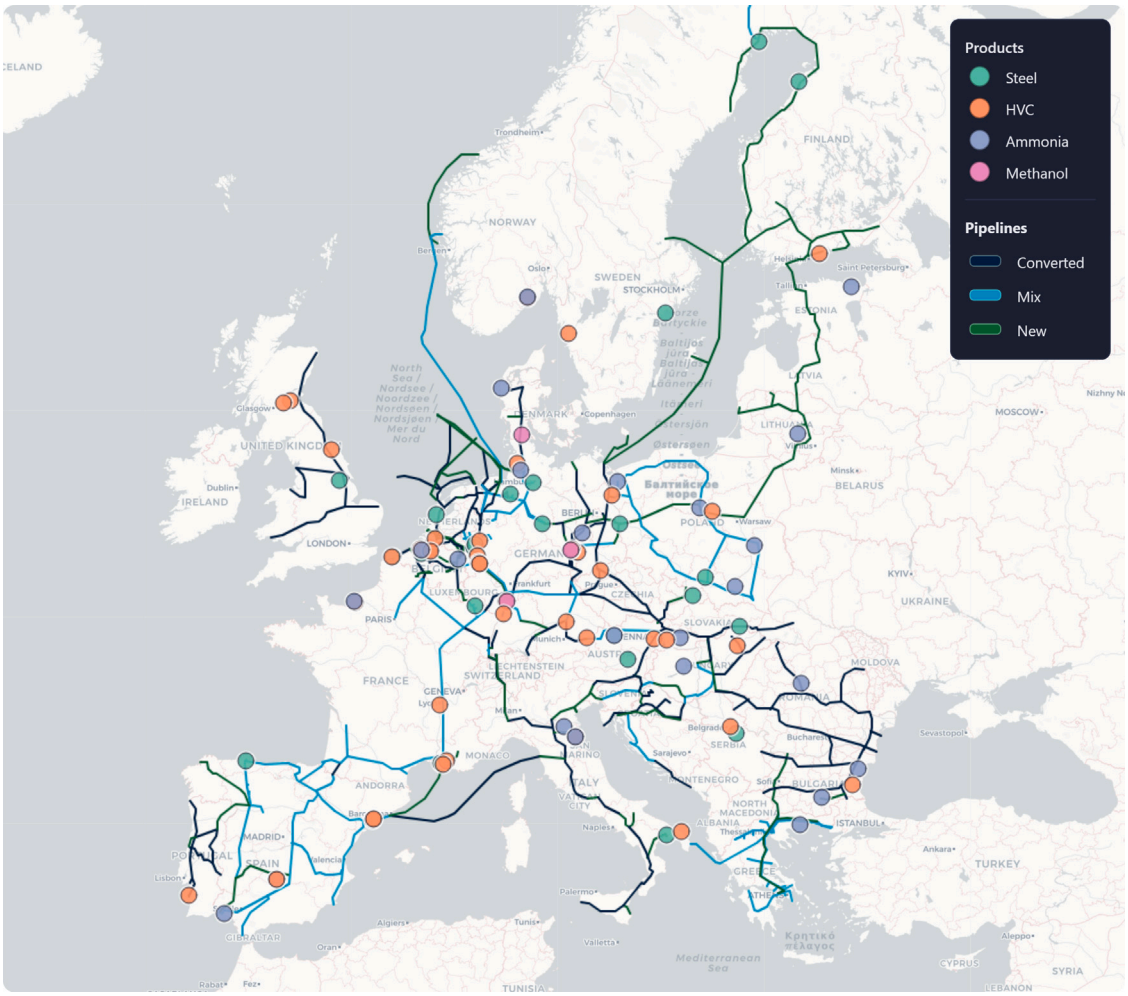


Fig. 3. Modelled primary steel and chemical production sites and projected European hydrogen pipeline network in 2050 based on the European Hydrogen Backbone.

Table 1
Techno-economic parameters and process-energy demand by product and process.
Source: [16].

Product	Process	CAPEX	Fixed OPEX	Electricity	Gas	Coal	Hydrogen
		€/(t/y)	€/t	MWh/t product			
Steel	BF–BOF	254.8	97.2	0.12	0.60	4.12	0.00
	BF–BOF (R)	93.4	97.2	0.12	0.60	4.12	0.00
	HDR–EAF	397.6	71.6	0.76	0.00	0.18	3.50
Ammonia	SR–HB	289.5	29.3	0.13	3.13	0.00	0.00
	SR–HB (R)	127.4	29.3	0.13	3.13	0.00	0.00
	H2–HB	432.3	21.6	1.72	0.00	0.00	0.00
Methanol	SR–MP	208.4	17.6	0.17	3.31	0.00	0.00
	SR–MP (R)	76.4	17.6	0.17	3.31	0.00	0.00
	H2–MP	172.9	8.6	1.50	0.00	0.00	0.00
HVC	NAPH–SCR	539.0	162.1	0.28	4.17	0.00	0.00
	NAPH–SCR (R)	197.6	162.1	0.28	4.17	0.00	0.00
	H2–MTO	1192.3	45.1	5.87	0.00	0.00	0.00

Notes: CAPEX and fixed OPEX are expressed in constant 2021 euros. Retrofit processes are denoted by "(R)". Energy demand refers to process-energy use only; non-energy feedstock demand is reported separately in Table 2. For the process-energy columns, Kaiser's methane and liquids energy-use inputs are aggregated under "Gas"; naphtha is retained separately only in the feedstock table. The integrated HVC route, denoted H2–MTO, combines on-site H2-based methanol production (H2–MP) with methanol-to-olefins production (MT–HVC).

3. Results

This section presents the baseline results and the sensitivity analyses, focusing on sectoral transformation pathways, hydrogen demand, emissions, and infrastructure investment.

3.1. Baseline scenario

The baseline scenario uses the techno-economic, energy-price, and infrastructure assumptions described above and serves as the central

Table 2
Feedstock demand of chemical production processes.
Source: [16].

Product	Process	Gas	Hydrogen	Naphtha
		MWh/t product		
Ammonia	SR–HB	5.83	0.00	0.00
	SR–HB (R)	5.83	0.00	0.00
	H2–HB	0.00	6.56	0.00
Methanol	SR–MP	6.94	0.00	0.00
	SR–MP (R)	6.94	0.00	0.00
	H2–MP	0.00	6.98	0.00
HVC	NAPH–SCR	0.00	0.00	11.81
	NAPH–SCR (R)	0.00	0.00	11.81
	H2–MTO	0.00	18.88	0.00

Notes: Retrofit processes are denoted by "(R)". Feedstock demand is reported in energy-equivalent terms using Kaiser's non-energy input convention. "Gas" corresponds to methane feedstock, while "Naphtha" corresponds to the non-energy liquids input for NAPH–SCR. For HVC, the H2–MTO route assumes on-site H2-based methanol synthesis followed by MT–HVC; the intermediate methanol requirement is therefore internalised and reported as hydrogen feedstock demand rather than methanol feedstock demand.

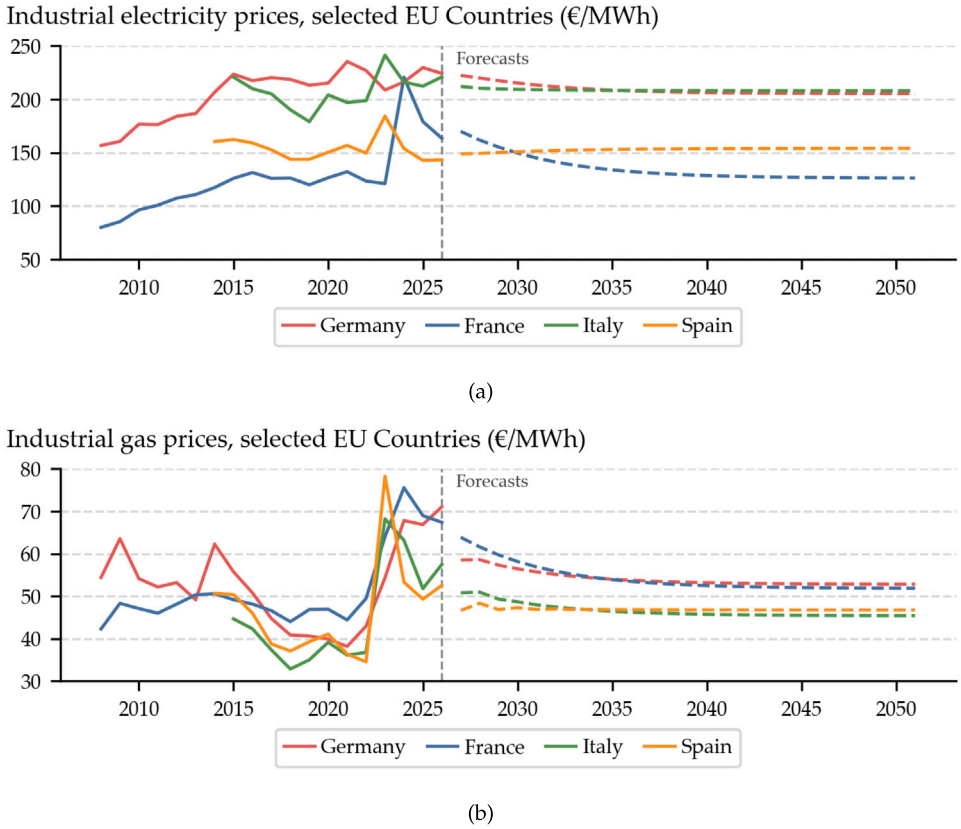


Fig. 4. Historical prices and modelled development of industrial electricity prices (a) and natural gas prices (b) for selected EU countries.

reference case for the analysis. It does not impose additional policy shocks or technology restrictions beyond the modelled evolution of energy prices, carbon prices, process costs, and hydrogen-network availability. Technology adoption therefore reflects the endogenous site-level investment logic of the model under central framework conditions. The two parameters introduced in Section 2.2, θ for premature process switching and η for shutdown decisions at reinvestment, are both set to 5%. The early-switching threshold prevents marginal cost differences from triggering frequent technology changes, while the reinvestment threshold requires a minimum cost advantage for continued operation.

Further, hydrogen pipeline connections are restricted to sites located within 100 km of an available pipeline segment. This threshold is intended as a modelling boundary to exclude implausibly long site-level connections rather than as a strict technical limit; implementation checks with alternative thresholds showed that substantially lower limits, particularly below approximately 80 km, excluded connections considered technically plausible, whereas higher limits mainly admitted increasingly long connections. Pipeline availability also includes an additional lead time beyond the commissioning year reported in the EHB data. We assume delays of 2 years for converted natural-gas infrastructure, 4 years for mixed infrastructure, and 6 years for new hydrogen pipelines. Accordingly, a segment becomes available to connected sites only after the corresponding delay.

Steel In the baseline, steel production declines only moderately, from about 84.3 Mt/y in 2025 to 75.4 Mt/y by 2050 (Fig. 5). The decline is selective: roughly 9.0 Mt/y of 2025 production exits, while 41 units, representing 75.4 Mt/y, remain in operation. Retirements are concentrated in older BF-BOF units in France, Austria, Slovakia, Poland, the United Kingdom, Germany, and Sweden. Surviving capacity

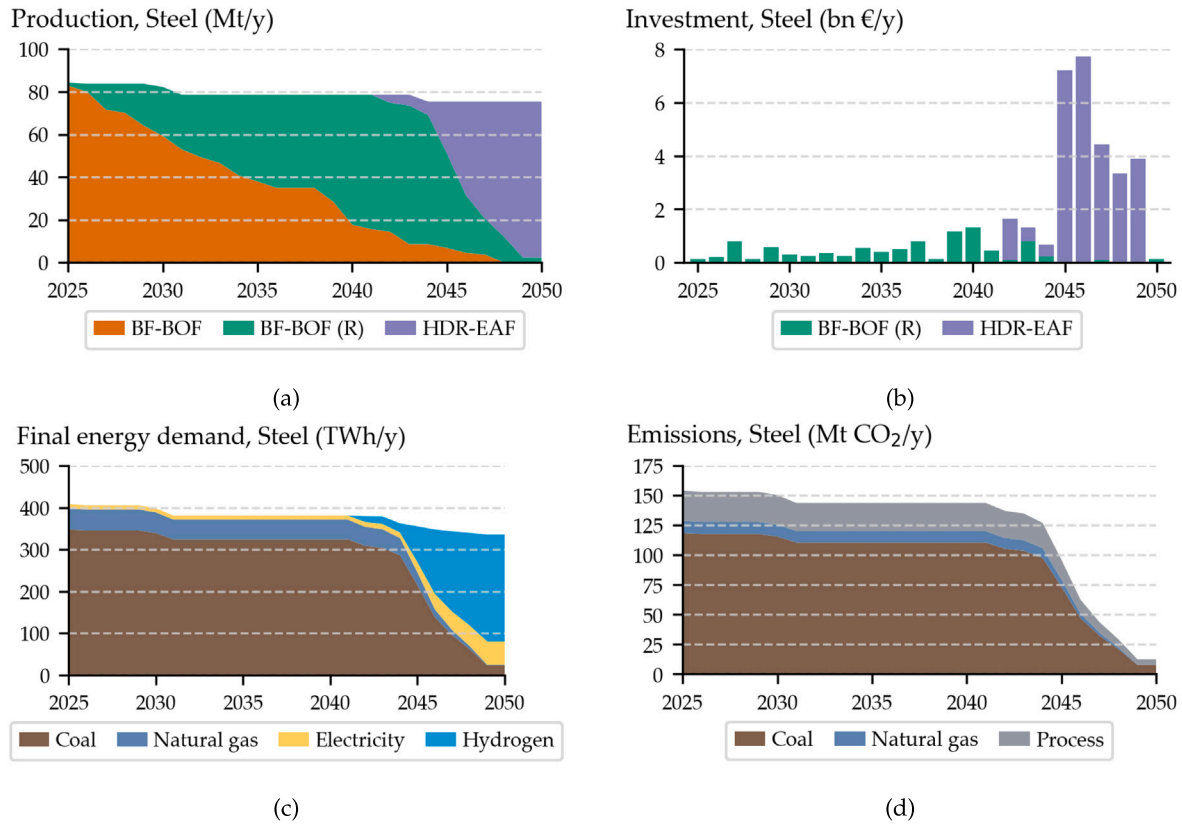


Fig. 5. (a) EU-wide development of primary steel production. (b) Investment in newly installed processes. (c) Corresponding development of energy demand. (d) Direct emissions.

is dominated by Germany, with substantial remaining volumes in the Netherlands, France, Belgium, Spain, Italy, Sweden, Austria, Finland, Poland, and Czechia. The main driver is asset vintage and reinvestment timing: retired units have an average last reinvestment year around 1988, compared with about 2016 for surviving units.

The investment pattern follows a two-stage pathway (Fig. 5). Through the 2030s and early 2040s, investment is mainly directed toward incremental BF-BOF retrofits. Once hydrogen infrastructure is accessible, deployment shifts rapidly toward HDR-EAF, with annual investment peaking at about 7.2–7.7 bn €/y in 2045–2046. However, the hydrogen network constraint leaves a small residual role for BF-BOF retrofits: two surviving units, about 2.3 Mt/y in total, remain on BF-BOF (R) in 2050 because their pipeline distances exceed the connection threshold. As a result, HDR-EAF reaches about 73.1 Mt/y by 2050 rather than fully replacing all surviving steel capacity.

The energy and emissions profiles therefore show a sharp late transition, but not complete elimination of fossil-based operation (Fig. 5). Coal use falls from about 347 TWh in 2025 to 23 TWh in 2050, while hydrogen rises to about 255 TWh and electricity to about 56 TWh. Emissions decline from roughly 154 Mt CO2/y in 2025 to about 12 Mt CO2/y in 2050, with the remaining emissions mainly associated with residual BF-BOF retrofit capacity. The baseline therefore describes a delayed and compressed steel transition, with hydrogen access determining which surviving units can complete the switch to HDR-EAF.

Ammonia In the baseline, ammonia production contracts from about 12.1 Mt/y in 2025 to 7.0 Mt/y by 2040, and remains broadly stable thereafter (Fig. 6). As in the case of steel, this decline reflects selective capacity retirement rather than a uniform reduction across the sector. Around 5.1 Mt/y of 2025 production exits by 2040, concentrated in a small number of large, older plants in Austria, the Netherlands, Germany, Italy, Belgium, Poland, Hungary, and Slovakia. Surviving capacity is more geographically dispersed, with the largest remaining volumes in Germany, Poland, and Lithuania. The main driver is reinvestment timing: retired units are larger and older on average, with a mean last reinvestment year around 2005, compared with about 2013 for surviving units.

Investment follows a staged transition (Fig. 6). Early spending is directed toward SR-HB retrofits, but only where reinvestment remains economically justified. From the early 2040s, investment shifts toward H2-HB as hydrogen-based ammonia becomes more competitive and hydrogen infrastructure access improves, with annual H2-HB investment peaking at about 0.6 bn €/y in 2043. The network-access constraint leaves a small residual role for gas-based production: about 0.41 Mt/y remains on SR-HB (R) in 2050, located in two units in France and Estonia whose hydrogen connection is not available within the distance threshold. H2-HB therefore reaches about 6.6 Mt/y by 2050, rather than fully replacing all surviving ammonia capacity.

The energy, feedstock, and emissions trajectories reflect both capacity selection and technology substitution (Fig. 7). Natural gas feedstock falls from about 67 TWh in 2025 to 2.4 TWh in 2050, while hydrogen feedstock rises to about 43 TWh. Final energy demand shifts from natural gas toward electricity, with electricity increasing to about 11 TWh by 2050 and residual natural gas falling to about 1.3 TWh. Total emissions decline from roughly 13.2 Mt CO2/y in 2025 to about 1.3 Mt CO2/y in 2050. The baseline therefore describes a smaller ammonia sector largely rebuilt around H2-HB, with a small residual gas-based segment where hydrogen access remains constrained.

Methanol In the baseline, methanol production remains constant at about 2.33 Mt/y from 2025 to 2050 (Fig. 8). The sector is small and highly concentrated: nine units remain in operation throughout the period, with seven German units accounting for about 2.29 Mt/y of output and two small units in Denmark and Iceland accounting for the

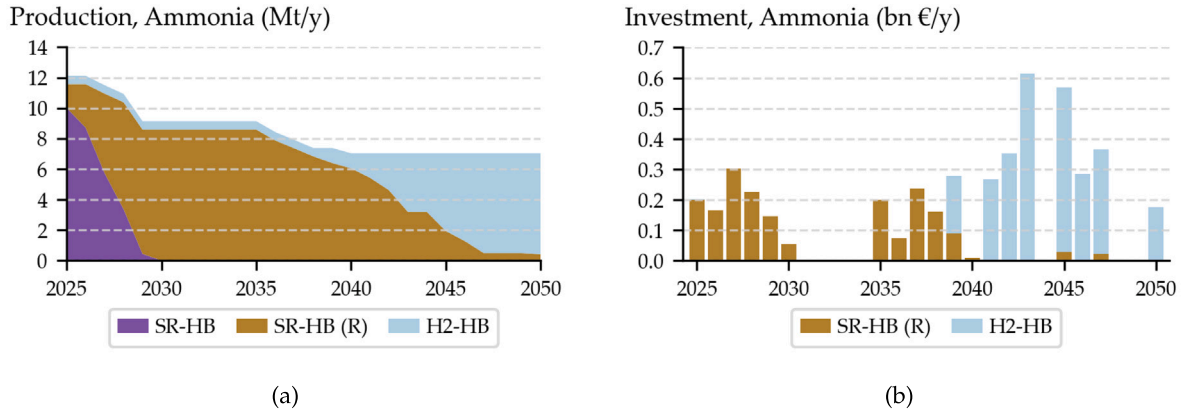


Fig. 6. EU-wide development of (a) ammonia production and (b) investment in newly installed processes.

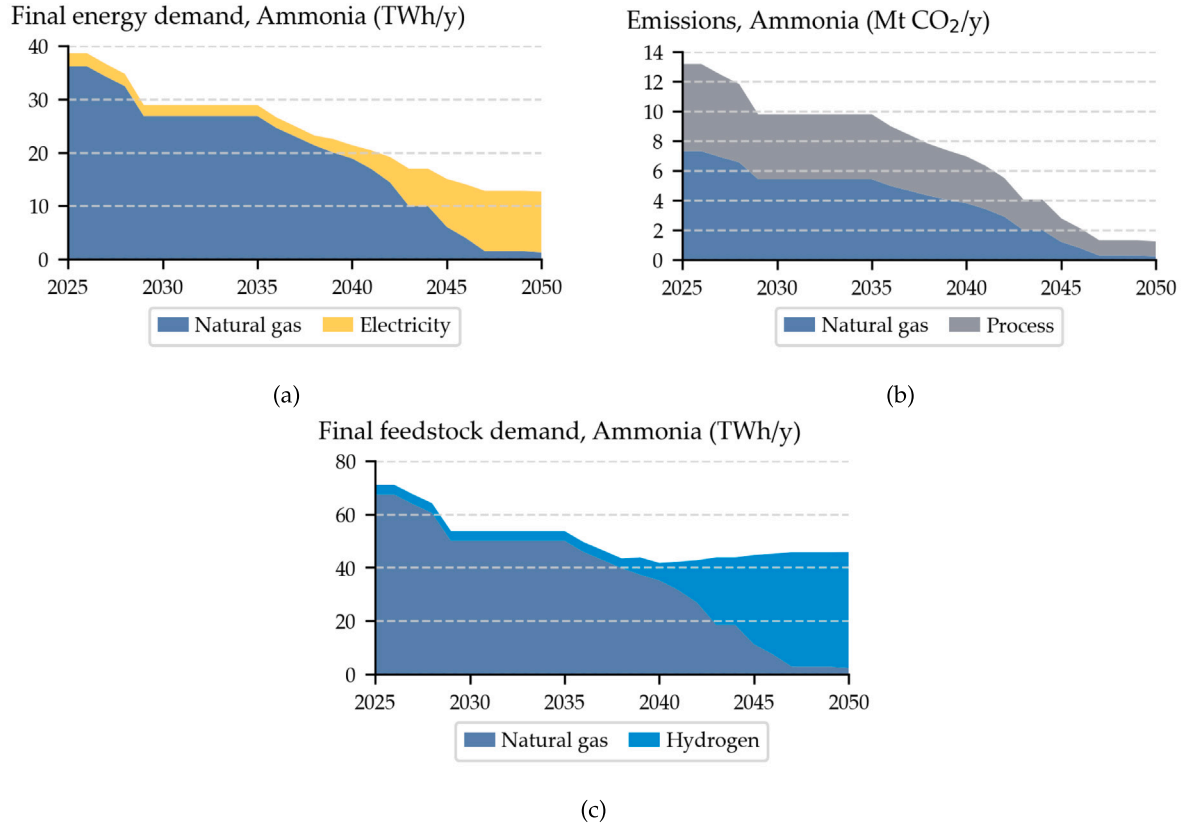


Fig. 7. EU-wide development of (a) energy demand, (b) direct emissions, and (c) feedstock demand in ammonia production.

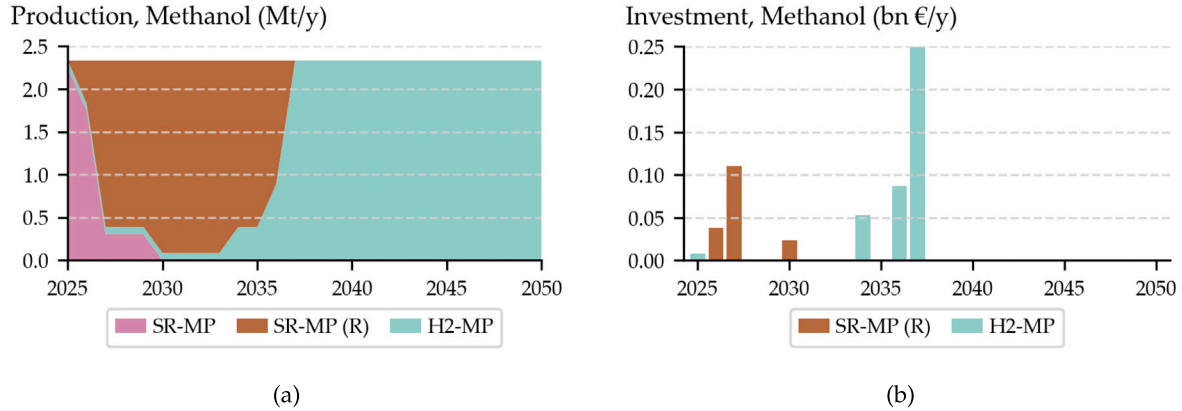


Fig. 8. EU-wide development of (a) methanol production and (b) investment in newly installed processes.

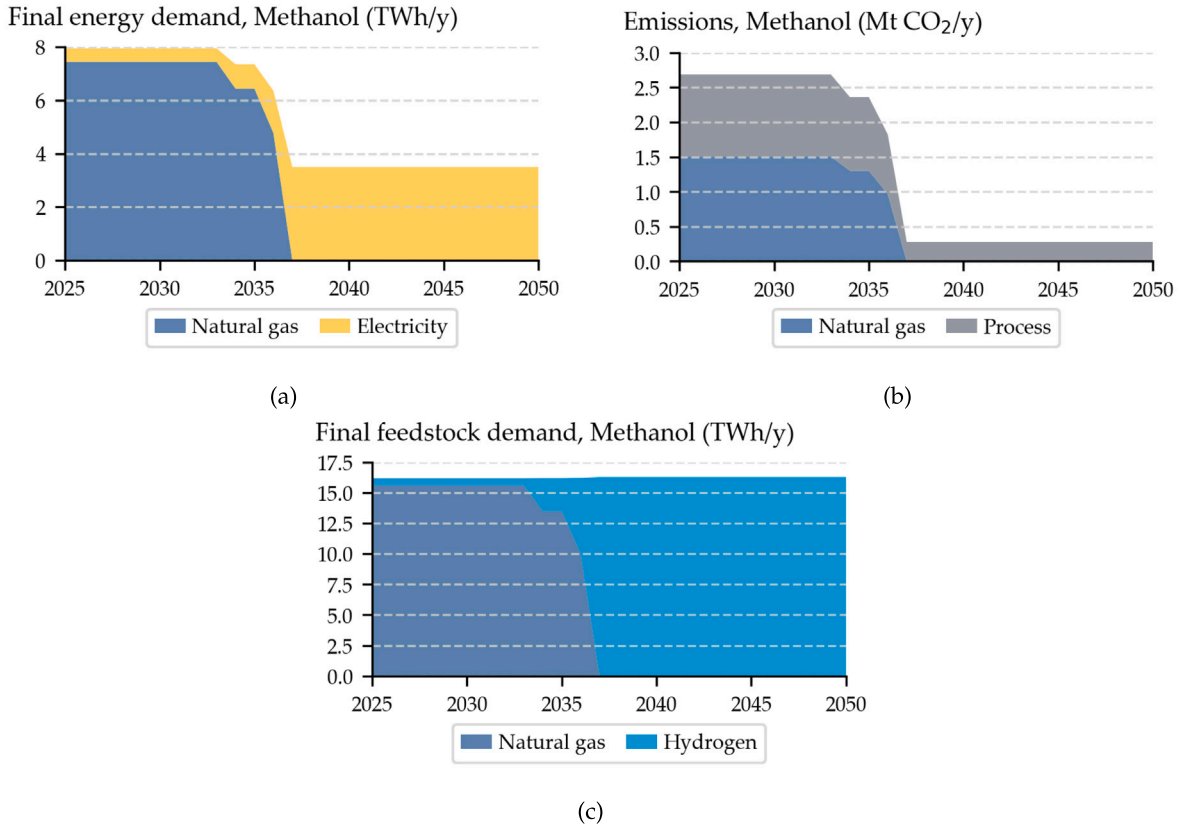


Fig. 9. EU-wide development of (a) energy demand, (b) direct emissions, and (c) feedstock demand in methanol production.

remainder. Five German SR-MP units represent almost all initially gas-based production, while four small H2-MP units are already present at the start of the simulation. The sectoral pattern is therefore not driven by capacity retirement, but by the synchronised conversion of a small number of German assets.

Investment occurs in two short phases (Fig. 8). Initial spending is directed toward SR-MP retrofits in the late 2020s, preserving the existing gas-based production base. A second, larger wave follows in the mid-2030s, when the main German units switch to H2-MP; annual investment peaks at about 0.25 bn €/y in 2037. This timing reflects the improving economics of hydrogen-based methanol production. H2-MP remains relatively costly at the start of the period, but its production cost falls from about 861 €/t in 2025 to about 654 €/t by 2037 and 515 €/t by 2050. The hydrogen network constraint does not leave residual gas-based capacity in this sector, so all methanol production is converted to H2-MP by 2037.

The energy, feedstock, and emissions trajectories show a complete fuel and feedstock substitution without any loss of output (Fig. 9). Natural gas feedstock falls from about 15.6 TWh in 2025 to zero after conversion, while hydrogen feedstock rises to about 16.3 TWh. Final energy demand shifts from roughly 7.5 TWh of natural gas in 2025 to about 3.5 TWh of electricity after 2037. Energy-related emissions are eliminated, and total emissions fall from about 2.7 Mt CO2/y in 2025 to around 0.3 Mt CO2/y from 2037 onward, reflecting residual process emissions. The methanol baseline therefore represents a compact, infrastructure-enabled conversion pathway rather than a restructuring or contraction of the sector.

HVC In the baseline, HVC production declines from about 20.6 Mt/y in 2025 to 17.9 Mt/y by 2030, and remains constant thereafter (Fig. 10). This contraction reflects the retirement of around 2.7 Mt/y of capacity, concentrated in a small number of units in Spain, Germany, Portugal, France, Slovakia, and Switzerland. Surviving production is geographically dispersed but led by Germany, Belgium, the United Kingdom, France, and the Netherlands. The vintage effect is present but weaker than in steel or ammonia: retired units have an average last reinvestment year around 2000, compared with about 2011 for surviving units. The dominant pattern is therefore not structural transformation, but continued operation of the incumbent naphtha-cracking route.

Investment is entirely directed toward NAPH-SCR retrofits (Fig. 10). The repeated investment peaks around 2026–2027, 2035–2037, and 2045–2047 reflect the 10-year retrofit lifetime rather than the deployment of a new low-carbon route. H2-MTO is not adopted because it remains far more expensive than continued naphtha cracking. Its capital cost is about 1190 €/t, compared with about 200 €/t for NAPH-SCR (R), and its annuity burden is more than three times higher. Although H2-MTO has lower base OPEX and lower process emissions, these advantages are outweighed by very high electricity and hydrogen requirements: 21.1 GJ/t of electricity and 68 GJ/t of hydrogen feedstock, compared with 1.0 GJ/t of electricity and 42.5 GJ/t of naphtha for the retrofit route. Even in 2050, H2-MTO production costs remain around 1555 €/t, compared with about 879 €/t for NAPH-SCR (R).

The energy, feedstock, and emissions profiles therefore remain essentially flat after the initial retirements (Fig. 11). Naphtha feedstock demand falls from about 243 TWh in 2025 to 211 TWh by 2030 and then remains unchanged. Final energy demand stabilises at roughly 75 TWh of natural gas and 5 TWh of electricity. Total emissions fall from about 33 Mt CO2/y in 2025 to around 29 Mt CO2/y by 2030, but do not decline further because the surviving sector remains naphtha-based. HVC is therefore the baseline outlier: hydrogen access does not induce fuel switching because the hydrogen-based route is structurally uncompetitive relative to repeated naphtha-cracker retrofits.

Hydrogen demand & pipeline investment In the baseline, industrial hydrogen demand remains limited through the 2030s but increases sharply

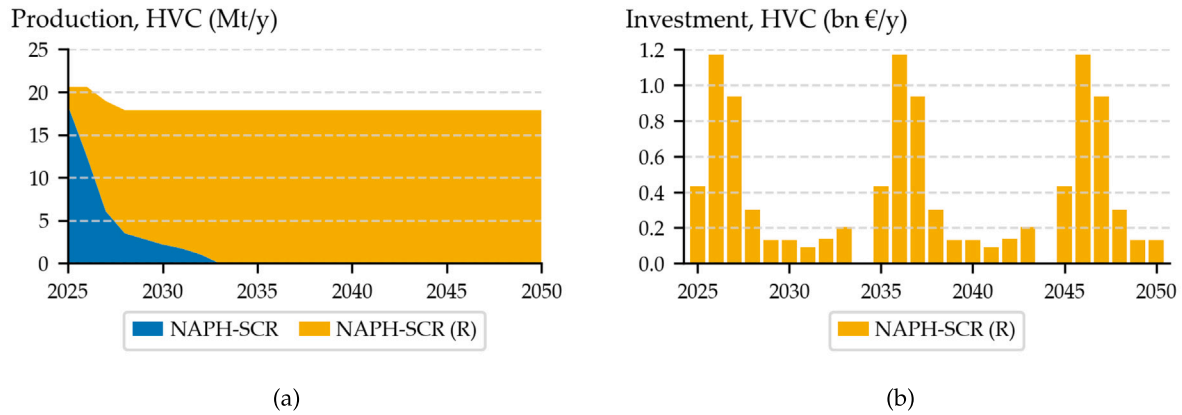


Fig. 10. EU-wide development of (a) HVC production and (b) investment in newly installed processes.

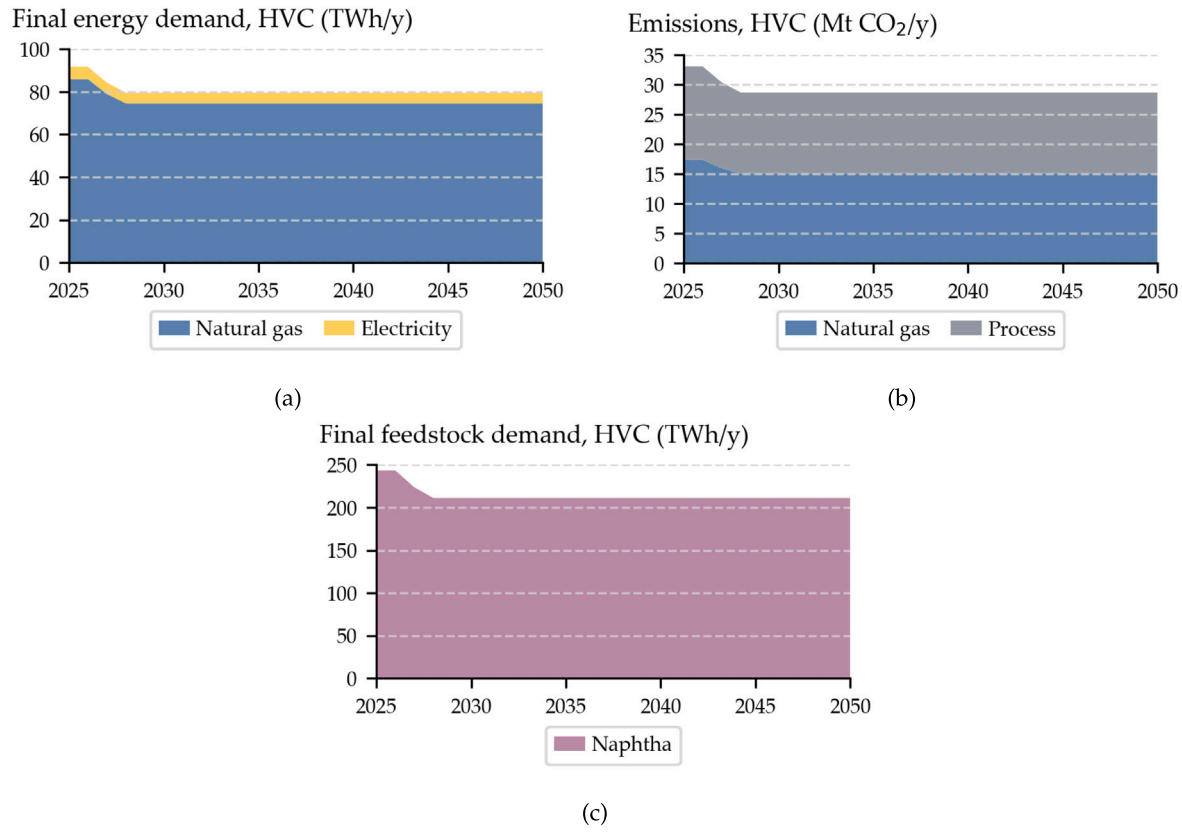


Fig. 11. EU-wide development of (a) energy demand, (b) direct emissions, and (c) feedstock demand in HVC production.

once large steel assets begin switching to HDR-EAF (Fig. 12). Total demand rises from 22.8 TWh/y in 2040 to 135.1 TWh/y in 2045 and 315.2 TWh/y in 2050. The early market is almost entirely chemical: chemicals account for 22.8 TWh/y in 2040, mainly ammonia and methanol. By 2050, however, steel dominates hydrogen use, reaching 255.5 TWh/y, or 81% of total demand, while chemicals contribute 59.7 TWh/y. The geography is correspondingly concentrated. Germany is the central hydrogen market, rising to 139.2 TWh/y in 2050, of which 110.7 TWh/y is steel and 28.5 TWh/y chemicals. The next largest markets are much smaller: the Netherlands 24.9 TWh/y, Spain 18.8 TWh/y, Poland 18.7 TWh/y, France 18.5 TWh/y, Belgium 17.5 TWh/y, Italy 14.5 TWh/y, and Austria 11.7 TWh/y.

Pipeline investment is therefore lumpy and anticipatory rather than proportional to aggregate hydrogen demand (Fig. 12). Cumulative pipeline expenditure is 306 mn € over 2025–2050, with 257 mn €, or 84%, occurring between 2039 and 2044. Annual expenditure peaks at 81 mn € in 2039 and 63 mn € in 2040, ahead of the main increase in hydrogen consumption after 2045. Mixed pipeline routes account for the largest share of cumulative spending, 159 mn €, followed by new hydrogen pipelines at 118 mn € and natural-gas pipeline conversion at 30 mn €. The country pattern reflects site-specific connection costs: Czechia has the highest cumulative investment, 58 mn €, despite modest 2050 hydrogen demand of 8 TWh/y, because the cost is dominated by the single Třinec steel site. Lithuania is similarly concentrated around the Achema ammonia plant, with 41 mn € of new-pipeline investment. Germany, by contrast, has by far the largest hydrogen demand but only 45 mn € of pipeline investment, indicating that several high-demand sites are relatively well positioned with respect to the assumed network. This asymmetry suggests that the main infrastructure challenge is not only the scale of national hydrogen demand, but the

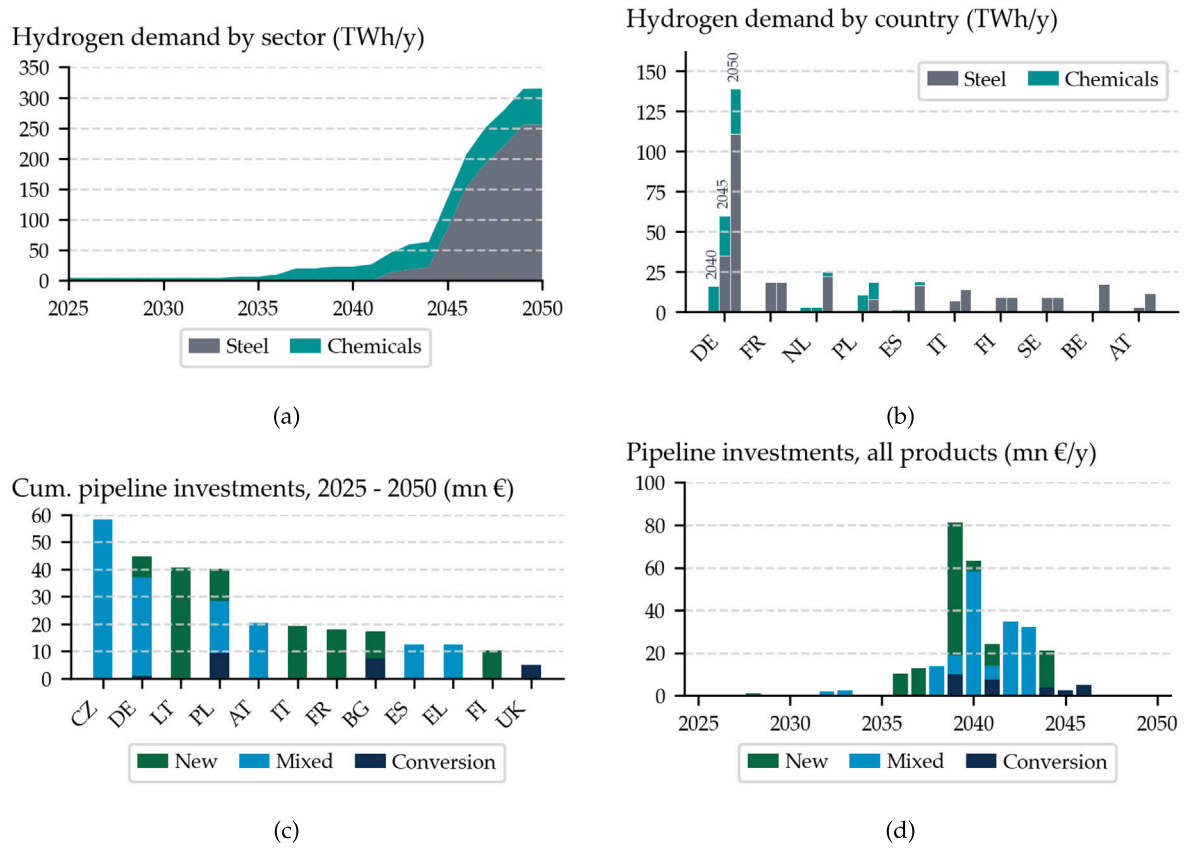


Fig. 12. (a) Hydrogen demand by sector over the simulation period 2025–2050. (b) Hydrogen demand by country and sector for the years 2040, 2045, and 2050. (c) Cumulative pipeline investment by country and connection type over the simulation period 2025–2050. (d) Annual pipeline investment by connection type over all modelled countries.

location of a small number of large industrial sites relative to feasible network connections.

3.2. Sensitivity analysis

To assess the robustness of the baseline results, four individual sensitivity analyses are conducted, complemented by two combined carbon- and hydrogen-price scenarios. These scenarios vary selected economic parameters while holding the underlying site structure, process data, reinvestment logic, and hydrogen-network assumptions constant. The first sensitivity examines the effect of higher CO_2 prices on the diffusion of low-emission production routes. The second varies hydrogen prices to test how strongly hydrogen-based processes respond to changes in fuel and feedstock costs. The third jointly varies electricity and natural-gas prices, capturing the interaction between electrified or hydrogen-based routes and fossil-based incumbent processes. Finally, an increased-economic-pressure scenario raises the reinvestment threshold η to examine whether less favourable competitiveness conditions lead to delayed technology adoption or capacity exit. Together, these sensitivities isolate the main economic drivers of technology diffusion and indicate which baseline findings are robust across alternative framework conditions.

Carbon price The high-carbon-price scenario examines how stronger carbon-cost pressure affects the diffusion of hydrogen-based production routes. Since carbon costs enter the operating cost of each process through both process-related and energy-related emissions, higher CO_2 prices increase the relative cost of fossil-based production and are expected to accelerate the adoption of low-emission alternatives. This scenario therefore tests whether carbon pricing primarily changes the timing of technology switching or also alters the long-run process mix. Following [19], the CO_2 price is assumed to rise to €300/tCO_2 by 2050. This scenario is intended as a sensitivity to substantially higher carbon costs rather than as a policy scenario, and no specific policy pathway for achieving this price level is assumed. All other techno-economic, energy-price, infrastructure, and decision-threshold assumptions remain unchanged relative to the baseline.

In steel, high carbon prices primarily accelerate the timing of decarbonisation rather than altering the 2050 endpoint (Fig. 13). HDR-EAF production rises to 72.9 Mt/y by 2045, compared with 24.4 Mt/y in the baseline, while 2050 output is nearly unchanged. This brings forward steel hydrogen demand from 85.4 to 254.8 TWh/y in 2045 and reduces steel emissions from 95.7 to 12.4 Mt CO2/y. The effect is concentrated in major steel-producing countries, including Germany, Austria, the Netherlands, Belgium, Spain, Poland, Italy, Slovakia, and the United Kingdom.

Ammonia also decarbonises earlier, though less strongly. H2-HB output increases from 1.0 to 2.4 Mt/y in 2040 and from 5.1 to 6.4 Mt/y in 2045, with additional uptake in countries such as Belgium, the Netherlands, Slovakia, Romania, and Bulgaria. Methanol is unchanged, while HVC shows only a small response: H2-MTO reaches 0.43 Mt/y in Finland by 2050, leaving almost all HVC production on the naphtha-based retrofit route. Overall emissions fall sharply in 2045, from 127.4 to 42.8 Mt CO2/y, but converge toward the baseline by 2050. High carbon prices therefore accelerate abatement, but are unlikely on their own to guarantee complete decarbonisation.

Hydrogen price The hydrogen-price sensitivity examines how uncertainty in future hydrogen supply costs affects the diffusion of hydrogen-based production routes. The low- and high-price cases are derived directly from the corridor-specific supply-cost assumptions reported by

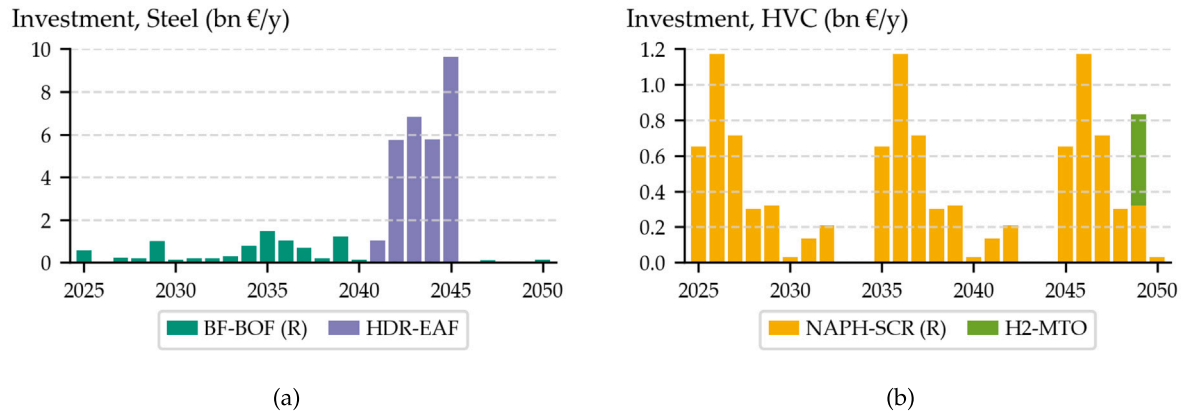


Fig. 13. Investment by process for (a) steel and (b) HVC in a scenario with elevated CO2 prices.

the European Hydrogen Backbone, while all other model parameters remain unchanged relative to the baseline. This sensitivity is particularly relevant because hydrogen enters both as an energy carrier in steel and as a feedstock in ammonia, methanol, and the H2–MTO route for high-value chemicals. The scenarios therefore test whether lower hydrogen prices mainly accelerate adoption where hydrogen-based routes are already close to competitiveness, or whether they fundamentally alter the sectoral pattern of technology diffusion.

Hydrogen price variation primarily affects the timing of fuel switching rather than the broad structure of the transition. In the Low Hydrogen Price scenario, total hydrogen demand rises earlier than in the baseline, reaching 70.4 TWh/y in 2040 and 229.2 TWh/y in 2045, compared with 22.8 and 135.1 TWh/y in the baseline. By 2050, however, the difference narrows, with hydrogen demand at 332.9 TWh/y compared with 315.2 TWh/y in the baseline. The High Hydrogen Price scenario has the opposite effect: hydrogen demand is delayed to 4.2 TWh/y in 2040 and 19.1 TWh/y in 2045, and remains lower in 2050 at 256.1 TWh/y.

Ammonia is the most price-sensitive sector. Under low hydrogen prices, H2-HB adoption is brought forward substantially, rising to 8.3 Mt/y by 2040 compared with 1.0 Mt/y in the baseline, with additional or earlier conversion concentrated in the Netherlands, Belgium, Slovakia, Germany, and Lithuania. Under high hydrogen prices, H2-HB deployment is delayed and reduced, reaching 5.6 Mt/y in 2050 compared with 6.6 Mt/y in the baseline, with the largest reductions in Germany, Lithuania, Bulgaria, and Romania. Steel also responds, but mainly through timing: low hydrogen prices increase HDR-EAF production in 2045 from 24.4 to 44.0 Mt/y, while high prices reduce 2050 HDR-EAF output from 73.1 to 58.0 Mt/y and leave more capacity in BF-BOF (R), particularly in France, Slovakia, and Germany. Methanol shows a temporary delay under high hydrogen prices, but converges to full H2-MP production by 2050. HVC remains essentially unaffected: even in the Low Hydrogen Price scenario, H2-MTO does not displace NAPH-SCR (R). The remaining cost gap is still large, about 531 €/t on a production-weighted basis in 2050, equivalent to a further hydrogen price reduction of roughly 7.8 €/GJ before H2-MTO reaches parity, holding other cost components fixed.

In sum, cheaper hydrogen accelerates decarbonisation where hydrogen-ready alternatives are already close to cost parity, especially ammonia and parts of steel, but it does not overturn process choices where hydrogen routes face structural penalties from high electricity demand and capital intensity.

Combined carbon & hydrogen price sensitivities The combined scenarios test whether carbon-price and hydrogen-price signals reinforce or offset one another. Both cases assume a CO_2 price of €300/tCO_2 in 2050, combined with either the low- or high-hydrogen-price trajectory; all other assumptions are retained from the baseline. The low-hydrogen-price case represents conditions favourable to hydrogen-based production, whereas the high-hydrogen-price case captures a more challenging hydrogen-cost environment under elevated carbon costs.

The low-hydrogen-price and high-carbon-price combination substantially accelerates hydrogen uptake. Total hydrogen demand reaches 172.4 TWh/y in 2040 and 333.0 TWh/y in 2045, compared with 22.8 TWh/y and 135.1 TWh/y in the baseline. By 2050, total demand reaches 353.8 TWh/y, compared with 315.2 TWh/y in the baseline. Ammonia responds strongly, with hydrogen demand increasing from 43.4 to 60.1 TWh/y and H_2–HB output reaching 9.2 Mt/y, compared with 6.6 Mt/y in the baseline. Steel remains dominated by HDR–EAF, which supplies 73.4 Mt/y, or 97% of steel output, in 2050. Methanol remains fully based on H_2–MP.

Importantly, the combined favourable case induces limited hydrogen uptake in HVC. H_2–MTO supplies 1.1 Mt/y in 2050, equivalent to 6.2% of HVC production, in Finland, France, and the Czech Republic. This requires 20.8 TWh/y of hydrogen feedstock demand. However, 93.8% of HVC output remains on the naphtha-based retrofit route. Thus, jointly favourable carbon- and hydrogen-price conditions can make H_2–MTO competitive at a small number of sites, but do not fundamentally alter the dominant HVC process mix by 2050.

Under high hydrogen prices combined with the elevated CO_2 price, HVC does not adopt H_2–MTO and remains fully reliant on NAPH–SCR (R). Total hydrogen demand nevertheless reaches 325.8 TWh/y in 2050, modestly above the baseline, reflecting the countervailing effect of stronger carbon-cost pressure. Hydrogen use reaches 261.8 TWh/y in steel and 51.3 TWh/y in ammonia, while methanol production and hydrogen demand fall to 1.8 Mt/y and 12.8 TWh/y, respectively. Overall, the combined sensitivities show that hydrogen prices and carbon prices interact strongly through the timing, scale, and location of hydrogen adoption. Cheap hydrogen under high carbon costs can accelerate deployment in ammonia and induce limited, late HVC adoption, whereas expensive hydrogen prevents H_2–MTO adoption even under high carbon prices.

Electricity & natural gas prices The energy-price sensitivity examines how joint variation in electricity and natural-gas prices affects technology diffusion. Rather than varying both carriers independently, the low- and high-price cases are derived from the dynamic factor model used for the baseline energy-price projections. This preserves the empirical co-movement between electricity and gas prices and therefore produces sensitivity cases that remain internally consistent with observed energy-market dynamics. To generate meaningful but realistic deviations from the baseline, the resulting scenarios imply average electricity

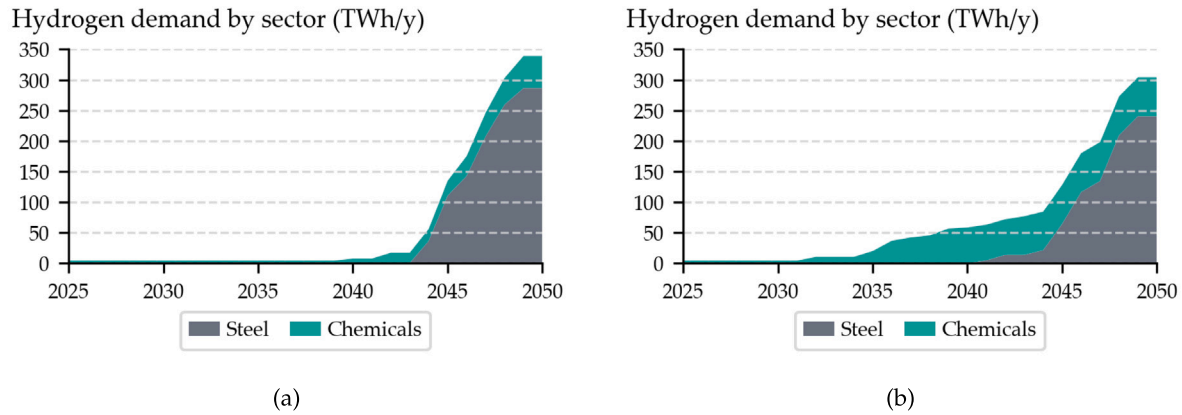


Fig. 14. Hydrogen demand by sector over the simulation period 2025–2050 in (a) Low Energy Price scenario and (b) High Energy Price scenario.

prices that are approximately 14% lower or higher than in the baseline in 2050, while average natural-gas prices are around 23%–25% lower or higher. The sensitivity therefore captures how coordinated shifts in energy-market conditions affect the relative competitiveness of fossil-based, electrified, and hydrogen-based production routes.

The energy-price sensitivity highlights the role of natural gas and electricity costs in determining both the timing and the extent of industrial hydrogen adoption (Fig. 14). In the Low Energy Price scenario, cheaper natural gas increases the attractiveness of fossil-based retrofits, particularly in steel and ammonia. Steel output is higher than in the baseline, reaching 84.2 Mt/y in 2050 compared with 75.4 Mt/y. However, HDR-EAF output is also higher in 2045, reaching 31.6 Mt/y compared with 24.4 Mt/y in the baseline. This occurs alongside greater BF-BOF (R) production, rather than a simple delay in steel hydrogen adoption. In ammonia, low gas prices favour SR-HB (R), reducing H2-HB output in 2045 from 5.1 Mt/y in the baseline to 1.8 Mt/y. These effects are concentrated in major steel-producing countries such as Germany, Austria, Slovakia, Poland, Italy, and France, and in ammonia-producing countries including Germany, the Netherlands, Poland, and Romania.

In the High Energy Price scenario, higher fossil-energy costs improve the relative attractiveness of hydrogen in ammonia. H2-HB output reaches 7.25 Mt/y in 2045, compared with 5.10 Mt/y in the baseline, while SR-HB (R) output falls to 0.41 Mt/y from 1.93 Mt/y. Steel responds differently: higher energy prices reduce total steel output to 71.1 Mt/y in 2050, compared with 75.4 Mt/y in the baseline, and HDR-EAF output falls to 18.4 Mt/y in 2045, compared with 24.4 Mt/y in the baseline. This indicates that higher energy prices can lead to capacity loss in steel rather than a straightforward shift toward HDR-EAF. HVC remains unchanged: H2-MTO production remains zero in 2045, while NAPH-SCR (R) accounts for 17.9 Mt/y in both the high-energy and baseline scenarios. Overall, the sensitivity shows that lower energy prices preserve incumbent routes, whereas higher energy prices increase hydrogen adoption in ammonia but can reduce both output and HDR-EAF deployment in steel.

The key implication is that energy-price changes affect both technology choice and industrial survival. Hydrogen adoption is therefore not a monotonic function of higher fossil-energy prices: beyond a point, cost pressure can induce exit rather than conversion.

Increased economic pressure The increased-economic-pressure scenario examines the effect of raising the reinvestment threshold parameter η from 5% in the baseline to 10%. This parameter determines whether a production unit continues operation when reinvestment is required: if the cheapest available process does not offer a sufficiently large cost advantage relative to the incumbent route, the unit is assumed to shut down rather than reinvest. Increasing the parameter η therefore represents a more demanding competitiveness environment, in which firms require a stronger economic case to justify continued operation. Conceptually, this may reflect higher exposure to international competition, tighter financing conditions, greater uncertainty about future demand, or stronger pressure to reduce production costs. The scenario thus tests whether decarbonisation under less favourable economic conditions leads mainly to delayed technology adoption or to capacity exit at marginal sites.

Relative to the baseline, steel output falls by 8.8 Mt/y in 2050, with HDR-EAF production declining from 73.1 to 64.3 Mt/y (Fig. 15). The additional loss is concentrated in Germany, Sweden, France, and Austria. These units are not prevented from adopting hydrogen technologically; rather, at their reinvestment points the switch to HDR-EAF yields cost reductions of only about 7%–9%, below the 10% threshold imposed in this sensitivity. The result is lower hydrogen adoption through capacity exit rather than delayed conversion. This lower steel capacity reduces cumulative steel investment from 38.7 to 34.9 bn €, hydrogen demand from 255.5 to 224.7 TWh/y, and final energy demand from 335.7 to 296.6 TWh/y in 2050. Emissions fall only slightly, from 12.4 to 11.4 Mt CO2/y, because the foregone production would largely have been hydrogen-based rather than coal-based.

Methanol shows a sharper capacity response. Output falls from 2.33 to 1.13 Mt/y after the mid-2030s, entirely due to German units that shut down rather than convert to H2-MP. As in steel, the relevant hydrogen switch is economically marginal: H2-MP reduces lifetime costs by only about 8%–10%, which is insufficient under the higher threshold. Consequently, methanol H2-MP investment falls from 0.40 to 0.19 bn €, hydrogen demand falls from 16.3 to 7.9 TWh/y, and emissions decline from 0.28 to 0.14 Mt CO2/y, mainly because production is lower.

Overall, the economic-pressure sensitivity mainly converts marginal decarbonisation investments into capacity exit. The transition therefore becomes smaller rather than slower: hydrogen adoption falls because fewer sites remain economically viable at the point of reinvestment.

4. Discussion

The results show that hydrogen-based transformation pathways differ sharply across steel and chemical subsectors. In the baseline scenario, total industrial hydrogen demand rises only gradually through the 2030s, but increases rapidly once large primary steel assets begin switching to HDR–EAF. By 2050, total hydrogen demand reaches 315.2 TWh/y, of which steel accounts for 255.5 TWh/y, or about 81%. Chemicals contribute 59.7 TWh/y, mainly through ammonia and methanol. This sectoral concentration is consistent with the broader literature, which identifies primary steel and ammonia as among the

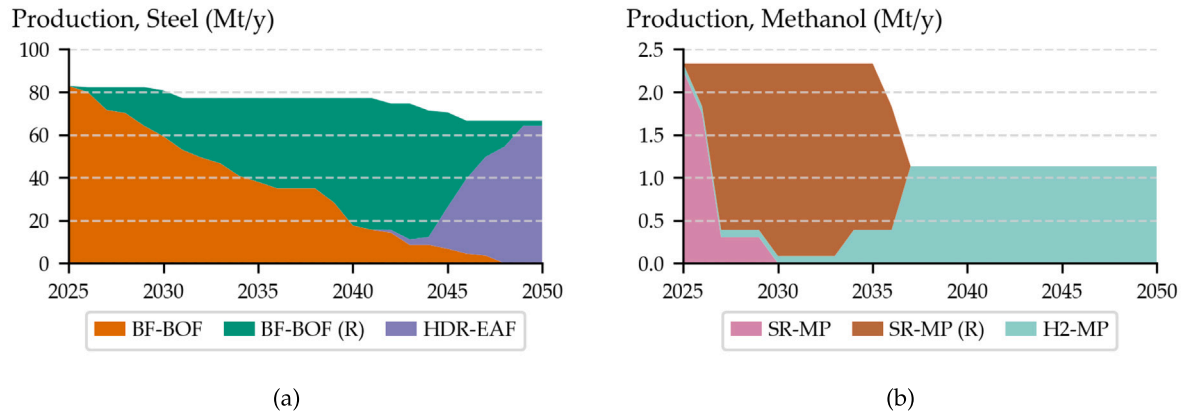


Fig. 15. Production by process for (a) steel and (b) methanol in the "increased economic pressure" scenario.

most plausible early large-scale industrial hydrogen users [13,31,32]. However, the result also demonstrates that hydrogen demand is highly scope-dependent: a model focused on primary steel and basic chemicals will necessarily produce a more hydrogen-intensive industrial pathway than economy-wide models that include a broader set of industrial energy uses (cf. [16,33]).

For steel, the baseline describes a delayed but compressed transformation, with surviving primary steel capacity shifting almost entirely from BF–BOF to HDR–EAF by 2050. The residual emissions are associated with remaining BF–BOF retrofit capacity at sites that cannot access hydrogen infrastructure within the modelled connection threshold. This finding is consistent with Schneider [4], who identifies hydrogen-based direct reduction as a central transformation route for steel production clusters in Northwestern Europe. At the same time, it should not be interpreted as a full steel-sector pathway. The model focuses on primary steel and does not endogenise scrap-EAF expansion, scrap quality constraints, or scrap trade. This matters because the wider literature expects scrap-based EAF production to provide a large share of future low-carbon steel, while clean primary production supplies the remaining demand [31,34,35]. In this sense, the steel hydrogen demand reported here is best understood as the demand associated with decarbonising the existing primary steel asset base, not as a prediction of total hydrogen use in a circular steel system. Given the restricted technology portfolio, the estimate is likely to lie toward the upper end of hydrogen demand associated with this asset base, since competing pathways such as CCS-based steelmaking or increased scrap use could displace part of the modelled hydrogen demand.

The comparison with [36] further clarifies this point. Their plant-level global steel model finds that energy-efficiency improvements and scrap reuse are the cheapest short-term abatement options, while smelt reduction with CCS becomes cost-effective after 2030 in many regions and green-hydrogen steelmaking contributes additional abatement in European plants after 2040. Our results are consistent with their emphasis on plant-level heterogeneity and the late emergence of hydrogen-based steelmaking, but differ in technology scope. Since the present model restricts the primary steel transition to BF–BOF retrofits and HDR–EAF, it does not allow CCS-based ironmaking, smelt reduction, or greater scrap substitution to compete with hydrogen. This modelling choice is appropriate for isolating hydrogen demand, but it likely narrows the set of cost-effective transition options. A broader technology portfolio would probably reduce hydrogen demand in some locations and delay hydrogen uptake where CCS or scrap-based routes are cheaper.

The chemical-sector results show a more differentiated pattern. Ammonia largely converts to H_2–HB by 2050, albeit with substantial capacity retirement and a corresponding shift from natural-gas to hydrogen feedstock. This illustrates the relatively direct role of hydrogen in ammonia decarbonisation: fossil hydrogen production is replaced by external low-carbon hydrogen, while the Haber–Bosch synthesis step remains intact. The result is therefore broadly aligned with studies that identify ammonia as the most straightforward hydrogen-based chemical transition route [17,18,37].

Methanol follows a different pathway, with production remaining constant while all gas-based production converts to H_2–MP by 2037. The model therefore identifies methanol as a compact, infrastructure-enabled conversion case. However, this result should be interpreted carefully. Methanol synthesis from hydrogen requires a carbon source, and the carbon neutrality of the resulting pathway depends on the origin, accounting, and availability of CO_2 or other carbon inputs [17,18]. The cost of sourcing sustainable carbon, for example from biogenic sources or direct air capture, is not explicitly represented in the H_2–MP operating costs. The present model focuses on site-level process choice and hydrogen demand, but does not endogenise sustainable carbon supply. Consequently, the methanol result is most robust as a hydrogen-demand estimate conditional on the assumed availability of suitable carbon feedstock.

High-value chemicals are the major outlier. H_2–MTO is not adopted in the baseline, and investment remains entirely directed toward repeated NAPH–SCR retrofits. This result is economically driven: even by 2050, H_2–MTO production costs remain around €1555/t, compared with about €879/t for NAPH–SCR (R). The cost gap reflects the high capital intensity and very high hydrogen and electricity requirements of the integrated H_2–MTO route. This result applies specifically to the H_2–MTO pathway represented here and does not preclude other potential applications of hydrogen in HVC production. More broadly, the chemicals literature emphasises that olefins and aromatics cannot be decarbonised by hydrogen substitution alone [17,38,39]. HVC decarbonisation likely requires a broader portfolio, including circular feedstocks, mechanical and chemical recycling, electrified cracking, biomass- or CO_2-based carbon sources, and demand-side material efficiency. Unlike in steel, however, these alternatives would primarily affect the decarbonisation pathway rather than reduce the baseline hydrogen-demand estimate, since H_2–MTO is not adopted in the baseline.

The sensitivity analysis shows that alternative price assumptions primarily affect transition timing and scale, while the dominant technology rankings remain comparatively robust. Higher carbon prices substantially bring forward HDR–EAF adoption while changing the 2050 endpoint comparatively little. Carbon pricing therefore acts primarily as a timing instrument: it accelerates fuel switching where hydrogen-based routes are already close to cost parity, but does not fundamentally alter the residual hard-to-abate structure. This is consistent with broader policy-model results showing that carbon pricing alone rarely closes industrial competitiveness gaps without complementary

instruments such as contracts for difference, green public procurement, product standards, infrastructure support, and border-adjustment mechanisms [31,33].

Hydrogen-price variation has a similar interpretation. By 2050, total hydrogen demand ranges from 256.1 TWh/y in the High Hydrogen Price scenario to 332.9 TWh/y in the Low Hydrogen Price scenario, compared with 315.2 TWh/y in the baseline. Ammonia is the most price-sensitive sector, while steel responds through both delayed adoption and, under high hydrogen prices, lower 2050 HDR–EAF deployment. HVC remains largely unaffected in the individual price sensitivities. Under the combined low-hydrogen-price and high-carbon-price case, however, H_2–MTO supplies 1.1 Mt/y, or 6.2% of HVC output, by 2050; the naphtha-based retrofit route nevertheless remains dominant. This indicates that lower hydrogen prices accelerate adoption where hydrogen routes are already near competitive, but overcome structural disadvantages in HVC only at a small number of sites when combined with strong carbon-cost pressure.

The economic-pressure sensitivity highlights a further risk: under stricter competitiveness thresholds, marginal decarbonisation investments turn into capacity exit rather than delayed transition. Increasing the reinvestment threshold η from 5% to 10% reduces 2050 steel output by 8.8 Mt/y and lowers steel hydrogen demand from 255.5 TWh/y to 224.7 TWh/y. Methanol output falls more sharply, from 2.33 Mt/y to 1.13 Mt/y, because several German units shut down rather than convert to H_2–MP. This result is important because many industrial pathway studies implicitly assume that incumbent production volumes remain in Europe. Recent work on green intermediate imports and industrial competitiveness suggests that, under high energy and hydrogen costs, Europe may instead import hydrogen-intensive intermediates such as HBI, ammonia, or methanol [40,41]. The present results are consistent with this concern: if hydrogen-based production does not provide sufficient cost reductions at reinvestment points, the model produces capacity loss rather than full domestic transformation.

Infrastructure plays a decisive but spatially uneven role. Cumulative pipeline-connection investment is modest relative to process investment, but highly lumpy and site-specific. Germany has the largest hydrogen demand in 2050, but relatively moderate pipeline investment because many high-demand sites are close to the assumed network. By contrast, countries such as Czechia and Lithuania face high connection expenditures concentrated around individual large sites. This asymmetry suggests that national hydrogen demand alone is an incomplete indicator of infrastructure challenge. What matters is the spatial coincidence of large industrial loads, pipeline corridors, connection distance, and timing of reinvestment. This supports the case for site-specific modelling and complements hydrogen-supply-chain studies that emphasise the need for coordinated infrastructure planning [42,43].

Several limitations follow from the modelling scope. First, hydrogen is treated as externally available at exogenous prices once infrastructure access is feasible. The model therefore does not endogenise upstream hydrogen production, electrolyser capacity, electricity-system constraints, storage, imports, or competition for hydrogen across sectors and countries. It also does not capture feedback from industrial demand growth to hydrogen prices. Binding upstream constraints could therefore increase delivered hydrogen costs, delay technology adoption, or reduce the hydrogen demand realised at individual sites relative to the modelled pathways. The resulting hydrogen-demand pathways should therefore be interpreted as conditional on the assumed hydrogen-price trajectories and infrastructure availability. Sector-coupled studies show that these upstream constraints can materially affect industrial pathways, especially when power, hydrogen, and synthetic-feedstock demand compete across sectors [16,44,45]. Moreover, recent spatially explicit analysis of European ammonia and methanol value chains likewise shows that the relative attractiveness of domestic production, hydrogen imports, and direct commodity imports varies strongly across industrial sites [15]. Second, the model assumes fixed production volumes except where shutdown occurs. It therefore does not represent demand-side material efficiency, substitution, trade relocation, or new site formation. Third, for sites whose capacities are reconstructed from EU ETS emissions, estimation errors introduce additional uncertainty into aggregate production and hydrogen-demand quantities. Since feedstock and energy demand scale with production volume, such errors primarily affect the magnitude of demand attributed to these sites rather than the underlying process-cost comparison, although they may be more consequential in smaller sectors with concentrated production. Fourth, the technology portfolio is deliberately hydrogen-centred. This clarifies hydrogen demand, but excludes potentially competing options such as CCS-based steelmaking, electrified steam cracking, bio-based chemical routes, carbon capture and utilisation, and expanded recycling. The resulting hydrogen demand should therefore be interpreted as conditional on the represented technology set rather than as total industrial hydrogen demand under a technology-neutral transition. Including these alternatives could reduce or delay hydrogen uptake where they are economically competitive. Fifth, investment decisions are deterministic. Firms observe modelled cost trajectories and do not face uncertainty over future energy prices, policy credibility, technology learning, or infrastructure delays. This perfect-information assumption may contribute to the concentrated timing of investment observed in the model, as multiple units can respond to the same anticipated changes in relative costs. Under uncertainty, heterogeneous expectations or more myopic decision-making could disperse investment over time, such that individual annual investment peaks should not be interpreted as precise forecasts of investment timing.

Despite these limitations, the analysis provides three robust insights. First, future industrial hydrogen demand is highly concentrated in a small number of sectors, countries, and sites. Second, reinvestment timing and infrastructure access strongly affect the temporal profile of hydrogen uptake; hydrogen demand can remain low for many years before rising rapidly once large assets reach economically favourable switching points. Third, hydrogen-based decarbonisation is not uniformly attractive across industrial processes. It is relatively compelling for ammonia and primary steel under favourable conditions, feasible for methanol conditional on clean carbon supply, and only marginally competitive in HVC even under jointly favourable carbon- and hydrogen-price conditions. These findings imply that policy should avoid treating industrial hydrogen demand as a homogeneous aggregate. Instead, hydrogen infrastructure planning, support instruments, and industrial-policy measures should be targeted toward site- and sector-specific transformation bottlenecks.

5. Conclusion

This paper shows that future industrial hydrogen demand in Europe is not simply a sectoral aggregate, but the outcome of spatially heterogeneous investment decisions. By modelling primary steel, ammonia, methanol, and HVC production at the level of individual sites and production units, the analysis shows that plant vintages, reinvestment timing, and hydrogen infrastructure access strongly shape both the timing and geography of hydrogen uptake. Within the hydrogen-centred technology portfolio considered, hydrogen demand remains modest for much of the simulation period, but rises sharply once large primary steel assets become economically and infrastructurally able to switch. The resulting transition is therefore lumpy, site-specific, and concentrated in a limited number of industrial regions.

The results also indicate that hydrogen is a highly uneven decarbonisation option across industrial processes. In primary steel and ammonia, hydrogen-based routes can become the dominant low-emission alternatives once infrastructure access and price conditions are sufficiently favourable. For methanol, their viability depends additionally on the availability of suitable carbon inputs. In HVC production, by contrast, hydrogen use through the MTO route is not adopted

in the baseline and becomes competitive only at a small number of sites under jointly favourable low-hydrogen-price and high-carbon-price conditions. Naphtha-cracker retrofits nevertheless remain the dominant route, indicating that the modelled H_2–MTO pathway is unlikely to provide a competitive decarbonisation route for this subsector. This distinction is crucial for industrial policy: treating hydrogen as a generic solution for hard-to-abate industry risks obscuring substantial process-level differences in cost structure, feedstock requirements, and infrastructure dependence.

Overall, the findings support a targeted rather than uniform hydrogen strategy for European industry. Infrastructure planning should prioritise large, well-defined industrial demand centres, while support instruments should be tailored to the economics of specific processes. For steel and ammonia, reducing hydrogen costs and coordinating pipeline access can materially accelerate fuel switching. For feedstock-intensive chemicals, however, hydrogen policy must be complemented by broader strategies for sustainable carbon supply, circular feedstocks, electrified process heat, and competitiveness protection.

Future work should therefore couple site-specific industrial diffusion models more closely with energy-system, trade, and circular-economy representations. A first priority is to improve the empirical basis of site-level industrial data, particularly with respect to plant capacities, process vintages, utilisation rates, retrofit options, and existing energy- and feedstock flows. More detailed process representations would also allow production units to face a broader set of technically feasible choices, including CCS-based routes, electrified steam cracking, bio-based feedstocks, synthetic carbon inputs, and recycling-based production pathways. This would move the model from a hydrogen-centred assessment toward a more comprehensive representation of industrial decarbonisation portfolios.

A second direction is to endogenise upstream energy and material constraints. Coupling site-specific industrial adoption to electricity-system, hydrogen-supply, storage, and import models would make it possible to assess whether the hydrogen and electricity required by industrial transformation are available at the assumed prices and locations. Similarly, linking the model to trade and circular-economy modules would allow future demand, relocation, material efficiency, and secondary production to affect site-level investment decisions rather than entering only through fixed production volumes or shutdown outcomes. Finally, future work should incorporate uncertainty more explicitly. Stochastic or adaptive investment formulations could account for uncertainty in energy prices, carbon prices, technology learning, infrastructure delays, and policy credibility, thereby providing a richer representation of the risks faced by industrial firms when committing to long-lived low-carbon assets.

CRediT authorship contribution statement

Anthony Britto: Writing – review & editing, Writing – original draft, Visualization, Validation, Software, Project administration, Methodology, Funding acquisition, Data curation, Conceptualization. **Leonie Gröning:** Writing – original draft, Validation, Methodology, Data curation. **Leandra Scharnhorst:** Writing – original draft, Validation, Supervision, Methodology, Funding acquisition, Conceptualization. **Max Kleinebrahm:** Writing – review & editing, Validation, Supervision, Project administration, Methodology. **Wolf Fichtner:** Writing – review & editing, Validation, Supervision, Project administration, Funding acquisition.

Declaration of competing interest

The authors declare that they have no known competing financial interests or personal relationships that could have appeared to influence the work reported in this paper.

Acknowledgements

AB and LS gratefully acknowledge financial support from Stiftung Energieforschung Baden-Württemberg under Grant FKZ A 348-22; parts of this work also appear in the project's final report. LS gratefully acknowledges financial support from Research Training Group 2153 of the German Research Foundation (DFG). The authors thank Noah Tröndle and Amirhossein Donyadidegan for excellent research assistance, and Marius Neuwirth for helpful discussions. The authors also thank three anonymous referees for helpful comments on the original manuscript.

Data availability

All data and code are published open source at https://gitlab.kit.edu/kit/iip/opensource/forecast-sites-ext.

References

[1] European Parliament and Council of the European Union. Regulation (EU) 2021/1119 of the European parliament and of the council of 30 june 2021 establishing the framework for achieving climate neutrality and amending regulations (EC) no 401/2009 and (EU) 2018/1999 (European Climate Law). Off J Eur Union 2021;L 243:1–17, URL: https://eur-lex.europa.eu/legal-content/EN/TXT/?uri=CELEX:32021R1119.

[2] Rózsai Máté, et al. JRC-IDEES-2023: The integrated database of the European energy system - data update and technical documentation. Tech report, Luxembourg: Publications Office of the European Union; 2026, http://dx.doi.org/10.2760/6945021.

[3] Lerede D, et al. Techno-economic and environmental characterization of industrial technologies for transparent bottom-up energy modeling. Renew Sustain Energy Rev 2021;140:110742. http://dx.doi.org/10.1016/j.rser.2021.110742.

[4] Schneider Clemens. Steel manufacturing clusters in a hydrogen economy – Simulation of changes in location and vertical integration of steel production in Northwestern Europe. J Clean Prod 2022;341:130913. http://dx.doi.org/10.1016/j.jclepro.2022.130913.

[5] Diesing Philipp, et al. From knowledge gaps to technological maturity: A comparative review of pathways to deep emission reduction for energy-intensive industries. Renew Sustain Energy Rev 2025;208:115023. http://dx.doi.org/10.1016/j.rser.2024.115023.

[6] van Rossum Rik, et al. A European hydrogen infrastructure vision covering 28 countries. Brussels: European Hydrogen Backbone; 2022, URL: https://ehb.eu/files/downloads/ehb-report-220428-17h00-interactive-1.pdf.

[7] Joas Fabian, et al. Klimaneutrale Industrie - Schlüsseltechnologien und Politikoptionen für Stahl, Chemie und Zement. de. Project report, Berlin, Wuppertal: Agora Energiewende, Wuppertal Institut für Klima, Umwelt, Energie; 2020, p. 236, URL: https://static.agora-energiewende.de/fileadmin/Projekte/2018/Dekarbonisierung_Industrie/164_A-EW_Klimaneutrale-Industrie_Studie_WEB.pdf.

[8] Bauer Fredric, Fontenit Germain. Plastic dinosaurs – Digging deep into the accelerating carbon lock-in of plastics. Energy Policy 2021;156:112418. http://dx.doi.org/10.1016/j.enpol.2021.112418, URL: https://linkinghub.elsevier.com/retrieve/pii/S0301421521002883.

[9] Bachorz Clara, et al. Averting the steel carbon lock-in through strategic green investments. Nat Clim Chang 2026;1–9. http://dx.doi.org/10.1038/s41558-026-02635-8, URL: https://www.nature.com/articles/s41558-026-02635-8.

[10] Capros Pantelis, et al. Outlook of the EU energy system up to 2050: The case of scenarios prepared for European Commission's "clean energy for all Europeans" package using the PRIMES model. Energy Strat Rev 2018;22:255–63. http://dx.doi.org/10.1016/j.esr.2018.06.009.

[11] Fleiter Tobias, et al. A methodology for bottom-up modelling of energy transitions in the industry sector: The FORECAST model. Energy Strat Rev 2018;22:237–54. http://dx.doi.org/10.1016/j.esr.2018.09.005.

[12] Guminski Andrej Philip Wolfgang. CO2 abatement in the European industry sector: Evaluation of scenario-based transformation pathways and technical abatement measures (Ph.D. thesis), Munich, Germany: Technical University of Munich; 2022, p. 173, URL: https://mediatum.ub.tum.de/1620112.

[13] Neuwirth Marius, Fleiter Tobias, Hofmann René. Modelling the market diffusion of hydrogen-based steel and basic chemical production in Europe – A site-specific approach. Energy Convers Manage 2024;322:119117. http://dx.doi.org/10.1016/j.enconman.2024.119117.

[14] Lerede Daniele, Di Cosmo Valeria, Savoldi Laura. TEMOA-Europe: An open-source and open-data energy system optimization model for the analysis of the European energy mix. Energy 2024;308:132850. http://dx.doi.org/10.1016/j.energy.2024.132850.

[15] Genge Lucien, et al. Optimising green value chains for the chemical industry in Europe. Int J Hydrog Energy 2026;199:152689. http://dx.doi.org/10.1016/j.ijhydene.2025.152689.
[16] Kaiser Markus, et al. Direct and indirect electrification in the German industry from a sector-coupled energy system modeling perspective. Energy Convers Manag: X 2025;28:101305. http://dx.doi.org/10.1016/j.ecmx.2025.101305, URL: https://www.sciencedirect.com/science/article/pii/S2590174525004374.
[17] Bazzanella Alexis Michael, Ausfelder Florian. Low carbon energy and feedstock for the European chemical industry. Tech. rep., Frankfurt am Main: DECHEMA Gesellschaft für Chemische Technik und Biotechnologie e.V. and The European Chemical Industry Council; 2017, URL: https://dechema.de/dechema_media/Downloads/Positionspapiere/Technology_study_Low_carbon_energy_and_feedstock_for_the_European_chemical_industry-p-20002750.pdf.
[18] Patonia Aliaksei, Poudineh Rahmatallah. Hydrogen for Chemical Industry. In: Patonia Aliaksei, Poudineh Rahmatallah, editors. Clean hydrogen for decarbonisation: beyond the 'next oil' narrative. Cham: Springer Nature Switzerland; 2026, p. 301–28. http://dx.doi.org/10.1007/978-3-032-19442-8_12.
[19] Neuwirth Marius, Fleiter Tobias, Hofmann René. Modelling the transformation of energy-intensive industries based on site-specific investment decisions. Sci Rep 2024;14(1):30552. http://dx.doi.org/10.1038/s41598-024-78881-7.
[20] Global Energy Monitor. Global iron and steel tracker. 2025, V1 Release. URL: https://globalenergymonitor.org/projects/global-iron-and-steel-tracker/.
[21] Global Energy Monitor. Global chemicals inventory. 2025, V1 Release, URL: https://globalenergymonitor.org/projects/global-chemicals-inventory.
[22] Fertilizers Europe. Industry facts and figures 2020. 2020, Brussels, URL: https://www.fertilizerseurope.com/wp-content/uploads/2020/07/Industry-Facts-and-Figures-2020-spreads.pdf.
[23] European Commission. Commission staff working document accompanying the communication "a European chemicals industry action plan". In: SWD(2025) 398 final. Brussels: European Commission; 2025-07-08, URL: https://eur-lex.europa.eu/legal-content/EN/TXT/?uri=CELEX:52025SC0398.
[24] Wang Anthony, et al. Analysing future demand, supply, and transport of hydrogen. European Hydrogen Backbone; 2021, URL: https://ehb.eu/files/downloads/EHB-Analysing-the-future-demand-supply-and-transport-of-hydrogen-June-2021-v3.pdf.
[25] European Commission and Eurostat. Producer prices in industry, total – annual data. Eurostat; 2026, http://dx.doi.org/10.2908/TEIIS010.
[26] Fulton Chad. Bayesian estimation and forecasting of time series in statsmodels. In: Proceedings of the 21st python in science conference. 2022, p. 83–9. http://dx.doi.org/10.25080/majora-212e5952-00d.
[27] European Commission and Eurostat. Gas prices for non-household consumers – bi-annual data from 2007 onwards. Eurostat; 2026, http://dx.doi.org/10.2908/NRG_PC_203.
[28] European Commission and Eurostat. Electricity prices for non-household consumers – bi-annual data from 2007 onwards. Eurostat; 2026, http://dx.doi.org/10.2908/NRG_PC_205.
[29] finanzennet. Naphtha in Euro und Dollar: Naphthapreis, aktueller Naphthakurs. 2026, Commodity price data for naphtha. URL: https://www.finanzen.net/rohstoffe/naphthapreis.
[30] ENTSO-E and ENTSOG. TYNDP 2024 scenarios: Final scenarios report. European Network of Transmission System Operators for Electricity and European Network of Transmission System Operators for Gas; 2025, Prepared by the joint Working Group Scenario Building team created by ENTSO-E and ENTSOG. URL: https://2024.entsos-tyndp-scenarios.eu/final-scenarios-report/.
[31] Choksey Ysanne, et al. Coal to clean: Climate-neutral steel by 2050. In: Policy Brief 382/06- P-2025/EN. Version 1.0. Agora Industry; 2025, p. 27, URL: https://www.agora-industry.org/publications/coal-to-clean-climate-neutral-steel-by-2050.
[32] Jayawardhana Purnima, Kiehle Julia, Calò Antonio, Pongrácz Eva. Hydrogen pipedreams or a new industrial revival: Industrial hydrogen demand by 2030 in Finland and europe. Renew Sustain Energy Rev 2025;222:115966. http://dx.doi.org/10.1016/j.rser.2025.115966.
[33] European Commission. Commission staff working document: Impact assessment accompanying the communication "stepping up Europe's 2030 climate ambition: Investing in a climate-neutral future for the benefit of our people". Tech. rep. SWD(2020) 176 final, Brussels: European Commission; 2020, URL: https://eur-lex.europa.eu/legal-content/EN/TXT/?uri=CELEX:52020SC0176.
[34] International Energy Agency. Iron and steel technology roadmap: Towards more sustainable steelmaking. Tech. rep., Paris: International Energy Agency; 2020, URL: https://www.iea.org/reports/iron-and-steel-technology-roadmap.
[35] Lee Daekyung, et al. Circular transformation of the European steel industry renders scrap metal a strategic resource. Resour Conserv Recycl Adv 2026;30:200323. http://dx.doi.org/10.1016/j.rcradv.2026.200323.
[36] Wu Xinyi, et al. Technological pathways for cost-effective steel decarbonization. Nature 2025;647:93–101. http://dx.doi.org/10.1038/s41586-025-09658-9.
[37] Ausfelder Florian, Herrmann Eghe Oze, López González Luisa Fernanda. Perspective Europe 2030: technology options for CO2-emission reduction of hydrogen feedstock in ammonia production. Tech. rep., Frankfurt am Main: DECHEMA Gesellschaft für Chemische Technik und Biotechnologie e.V; 2022.
[38] International Energy Agency. The future of petrochemicals: Towards more sustainable plastics and fertilisers. Tech. rep., Paris: International Energy Agency; 2018, URL: https://www.iea.org/reports/the-future-of-petrochemicals.
[39] Münnich Paul, et al. Chemicals in transition: The three pillars for transforming chemical value chains. In: 300/04-I-2023/EN. Version 1.2. Agora Industry; 2023, p. 55, URL: https://www.agora-industry.org/publications/chemicals-in-transition.
[40] Seibold Toni, et al. Balancing cost savings and import dependence in Germany's industry transformation. 2025, http://dx.doi.org/10.48550/arXiv.2510.00918.
[41] Di Bella Alice, et al. Pursuing decarbonization and competitiveness: a narrow corridor for European green industrial transformation. 2025, http://dx.doi.org/10.48550/arXiv.2510.08199.
[42] Ganter Alissa, et al. Minimum-regret hydrogen and carbon supply chains to decarbonize European industrial hydrogen demands. Environ Sci Technol 2025;59(28):14372–87. http://dx.doi.org/10.1021/acs.est.4c13659.
[43] Slowinski Robert, et al. Implementation roadmap: Cross border projects and costs update. Tech. rep., Brussels: European Hydrogen Backbone; 2023, URL: https://ehb.eu/files/downloads/EHB-2023-Implementation-Roadmap-Part-1.pdf.
[44] Raillard-Cazanove Quentin, Knibiehly Thibaut, Girard Robin. Decarbonisation of industry and the energy system: Exploring mutual impacts and investment planning. J Clean Prod 2025;508:145511. http://dx.doi.org/10.1016/j.jclepro.2025.145511.
[45] Mayer Patricia, et al. Transition pathways to electrified chemical production within sector-coupled national energy systems. Energy Environ Sci 2025;18:7967. http://dx.doi.org/10.1039/D5EE01118C.